x-ray imaging at the nanoscale / mit Röntgenaugen im Nanokosmos unterwegs

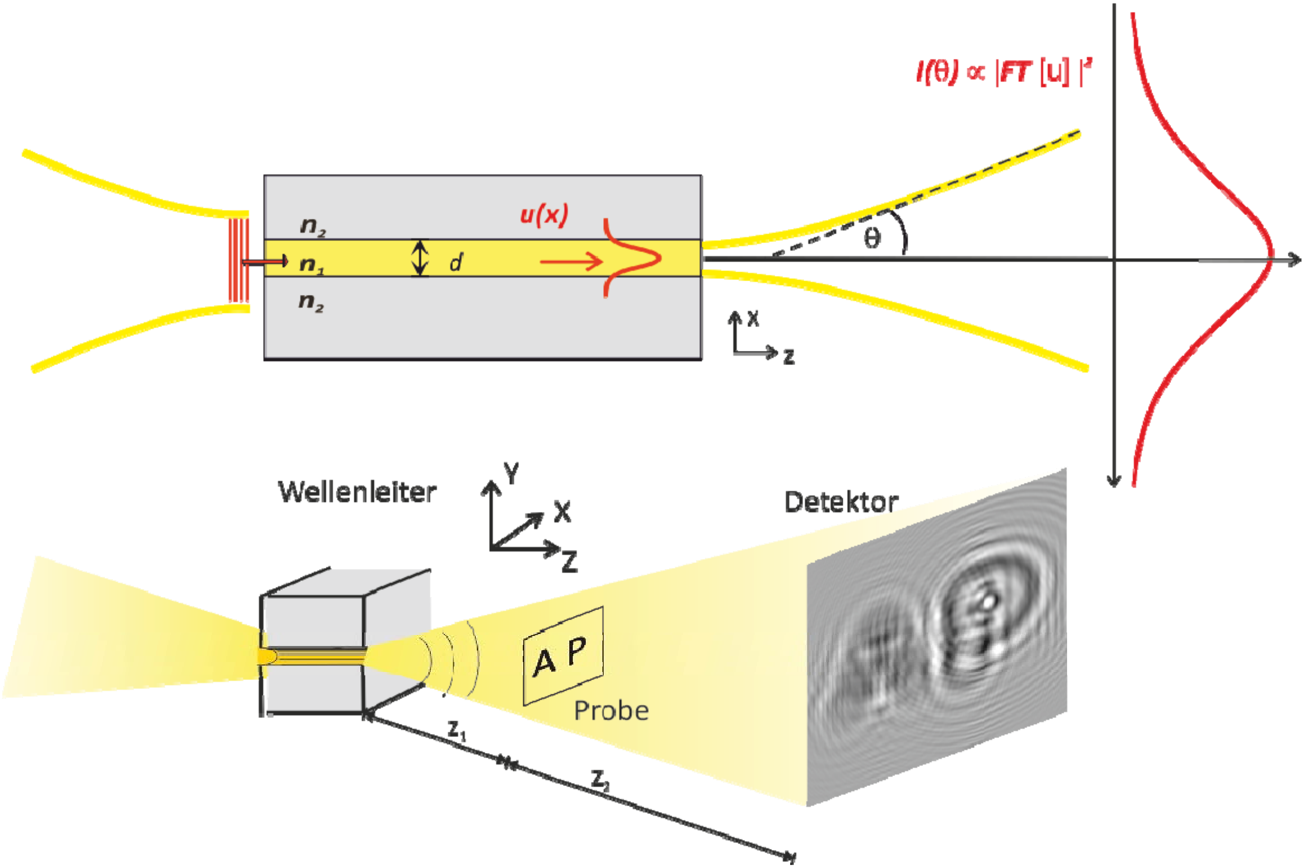

Tim Salditt, Institut für Röntgenphysik
joint work with Matthias Bartels, Robin Wilke, Marius Priebe
Klaus Giewekemeyer, Markus Osterhoff
Universität Göttingen,

Physik-Kolloquium Oldenburg, 7.11.2011

SFB 755

Content

1. Why x-ray imaging ?
2. The phase problem and its solution by iterative phasing
3. **far-field (CDI) versus near-field (propagation) imaging**
4. **The Göttingen endstation for nano-imaging**
   at the coherence beamline PETRAIII HASYLAB /DESY
5. **X-ray waveguide optics**
6. **Applications in biological imaging**
7. The advent of X-ray Free Electron Lasers (XFEL)

joined work with
Matthias Bartels, Robin Wilke, Marius Priebe, Markus Osterhoff, Sebastian Kalbfleisch
Scen Krüger, Henrike Neubauer, Dr. Klaus Giewekemeyer

1. Imaging with x-rays- advantage No.1: transparency

$$I(z) = I_0 e^{-\mu z}$$

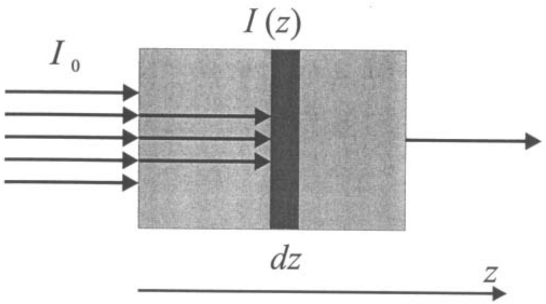

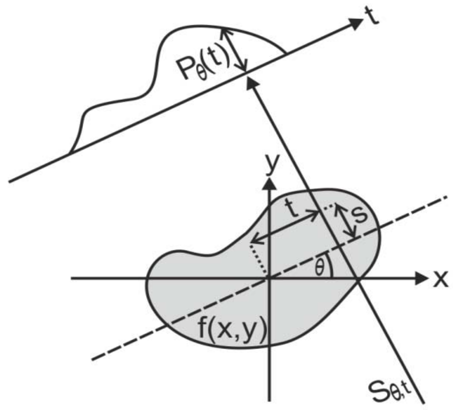

tomography

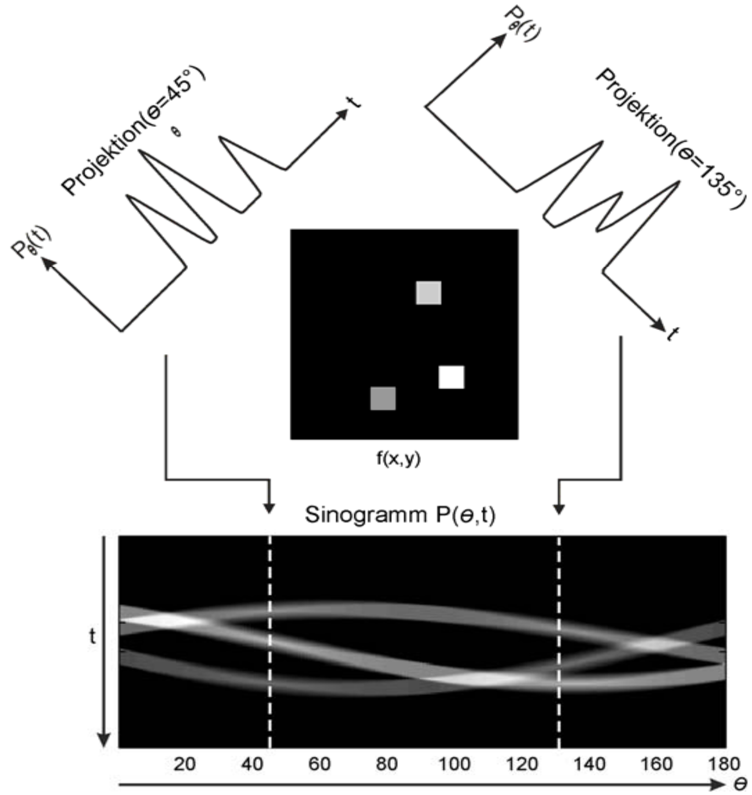

absorption coefficient μ~E^{-3} Z^{-4}

look into biomaterials

(bulk information)

absorption versus phase contrast

$$n = 1 - \delta + i\beta$$

x-ray index of refraction

$$u(x,y) = u_0(x,y) \quad \tau(x,y)$$

$$\tau(x,y) = \exp[-k \int_z^{z+d} dz \; (\beta(x,y,z) + \mathrm{i}\delta(x,y,z))]$$

$\delta = 10^{-5} \,..\, 10^{-9}$

$\beta = 10^{-7} \,..\, 10^{-13}$

Absorption length μ

$$\beta = \frac{\mu}{2k}$$

Phase shift

$$\Delta\phi = k\,\Delta d(1-n)$$

slab with index n

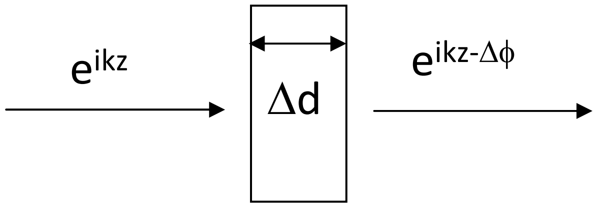

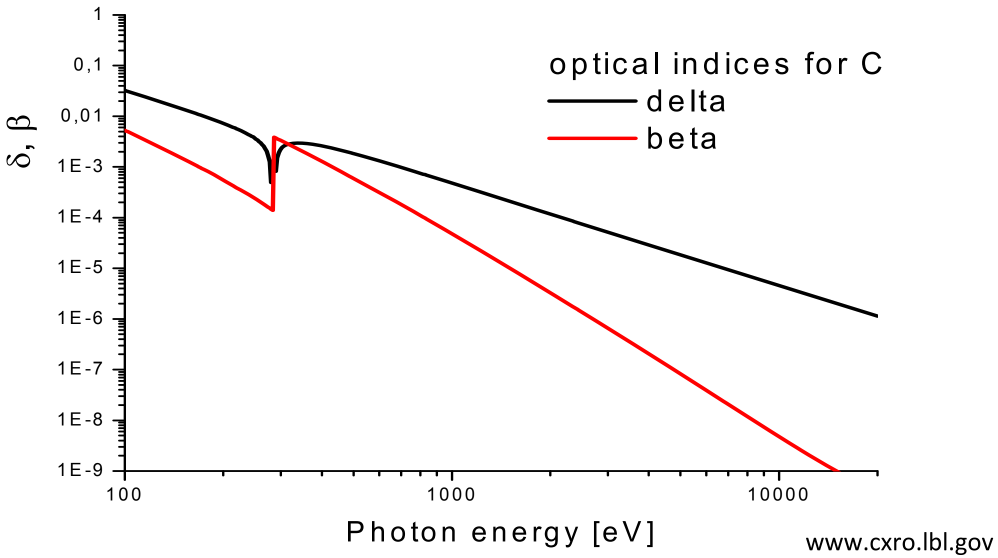

$\delta \gg b$ for low Z elements and high photon energies → phase contrast

Propagation imaging

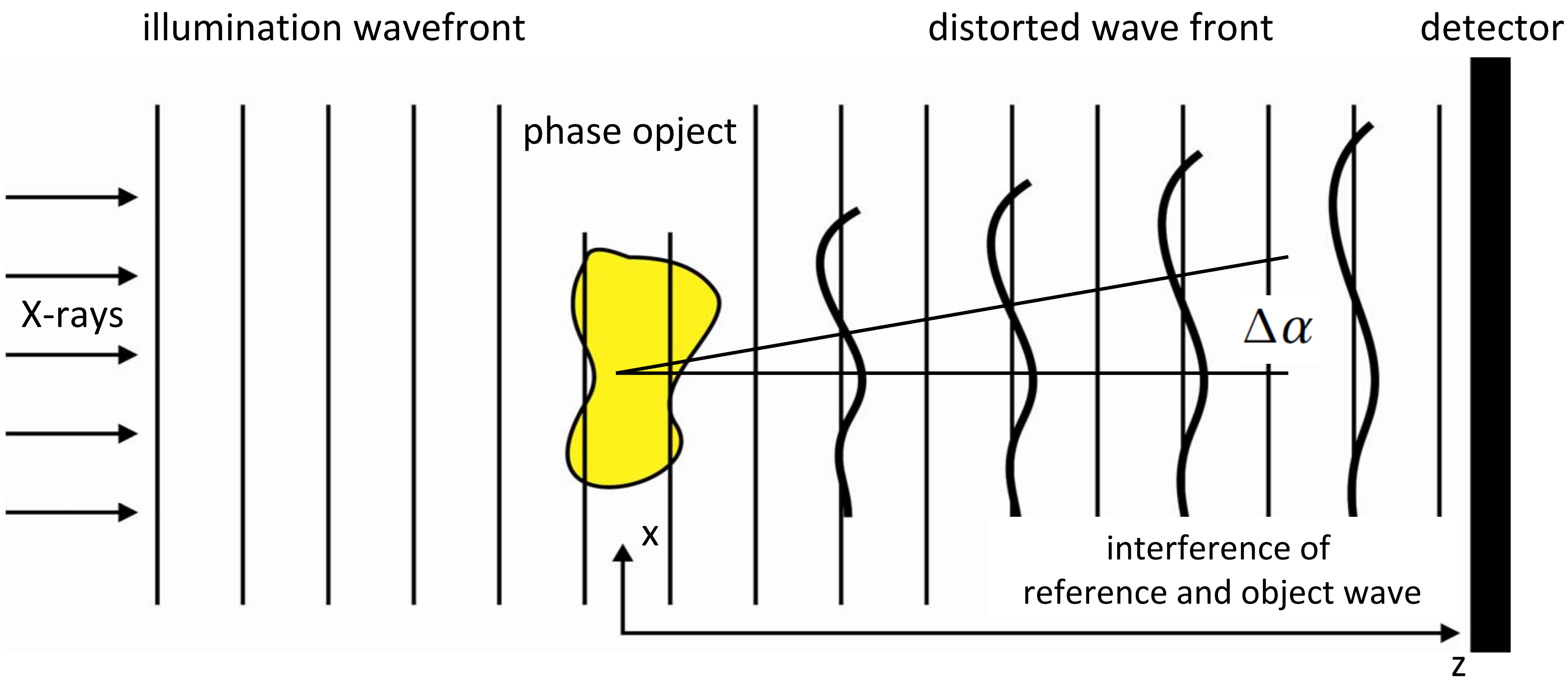

phase shift $\Delta\phi = k\,\Delta d\,(1-n)$

free space propagation

slab with index n

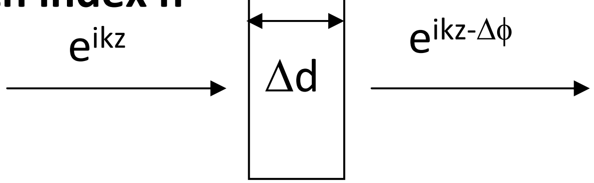

$$\Delta\alpha = \frac{\lambda}{2\pi}\frac{\partial\phi}{\partial x}$$

P. Cloetens et al. et al. ,1999; S.Wilkins et al. , 2000-2004

Density in 3D : resolution AND contrast matter !

Cochlea: Phase contrast vs. Absorption contrast

M.Bartels et al., unpublished

X-ray advantage No.2:
(a) quantitative contrast and weak scattering cross section

index $n = 1 - \delta + i\,\beta$, $\delta, \beta \approx 10^{-5}$-$10^{-6}$
close to 1.
$\Rightarrow$ reduced reflections at internal interfaces

no multiple scattering

(look through foam of beer, R.W. Pohl 1939)

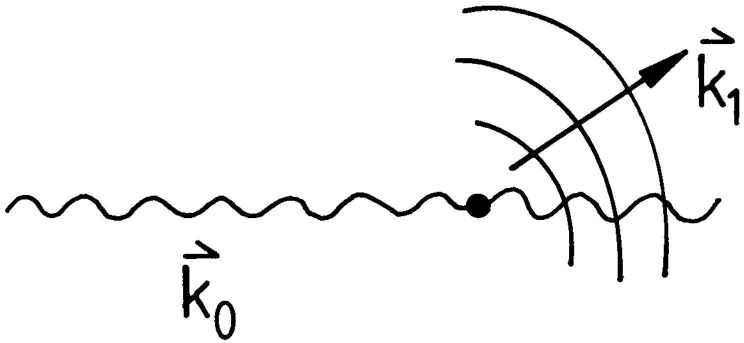

$$e^{i\vec{k}_0\cdot\vec{r}} \longrightarrow e^{i\vec{k}_0\cdot\vec{r}} + f(\Omega)\,\frac{e^{ik_0\cdot r}}{r}$$

$f(\Omega)$ amplitude, $[f(\Omega)] = m$ „scattering length “
$f = 2.82\ 10^{-15}$ m

(Born Approx.)

crystallography = averaging over 10^{12} - 10^{18} copies of the same molecule

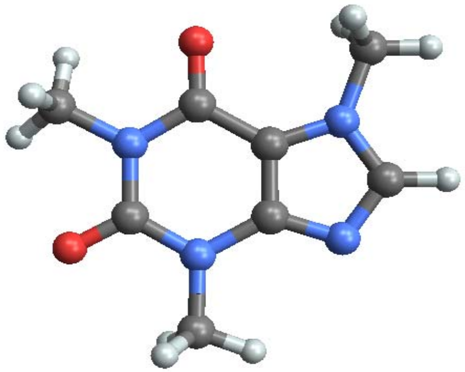

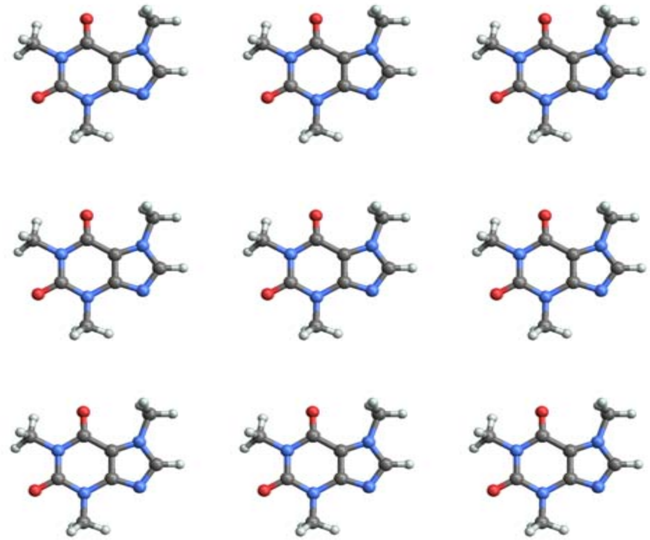

$$S(\vec{q}) = \left|\sum_{unit\ cell}^{N} e^{i\vec{q}\cdot\vec{r}_n}\right|^2 \left|\sum_{n_1 n_2 n_3} e^{i\vec{q}\cdot\left(n_1\vec{a}+n_2\vec{b}+n_3\vec{c}\right)}\right|^2$$

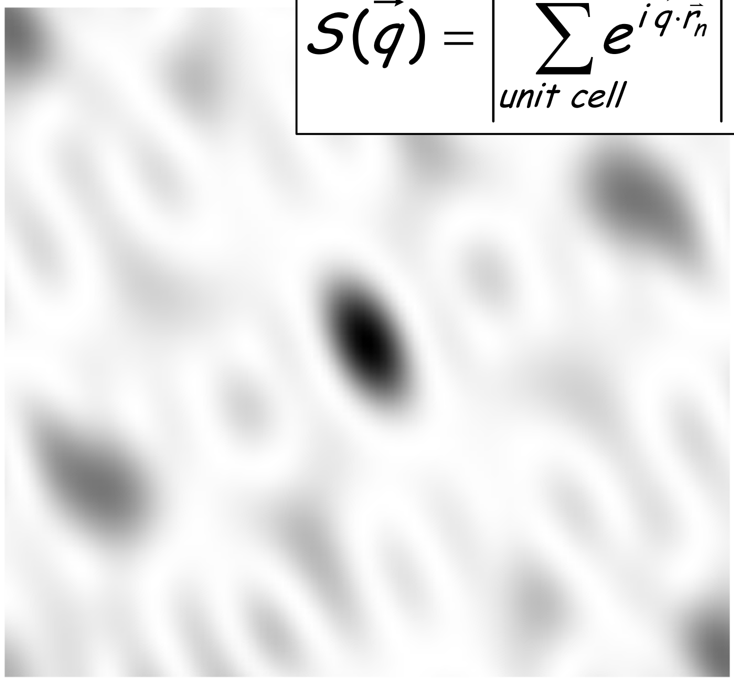

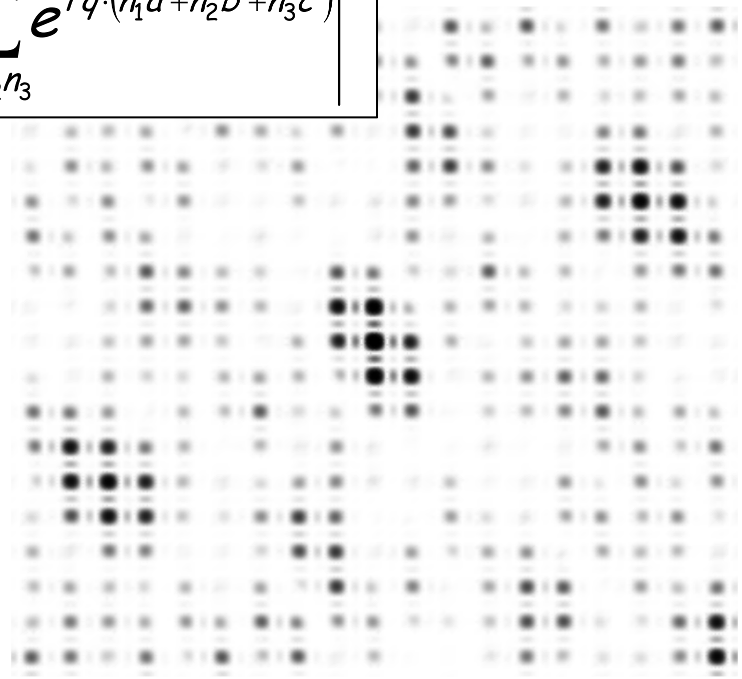

Advantage No.3: small wavelength – high resolution

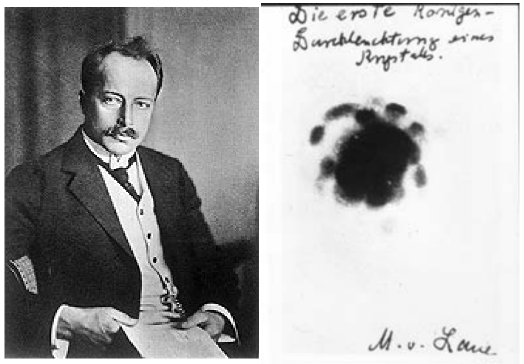

Max .v. Laue 1912

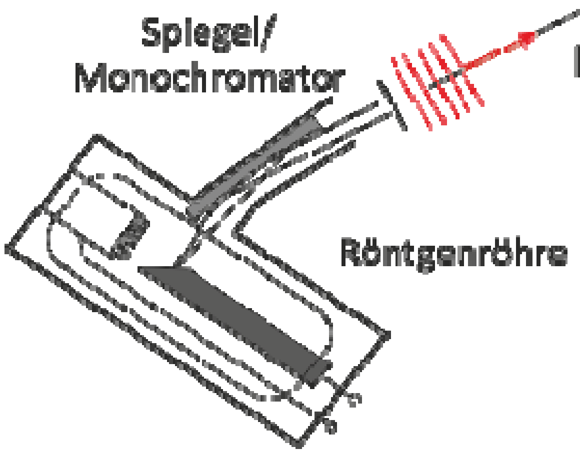
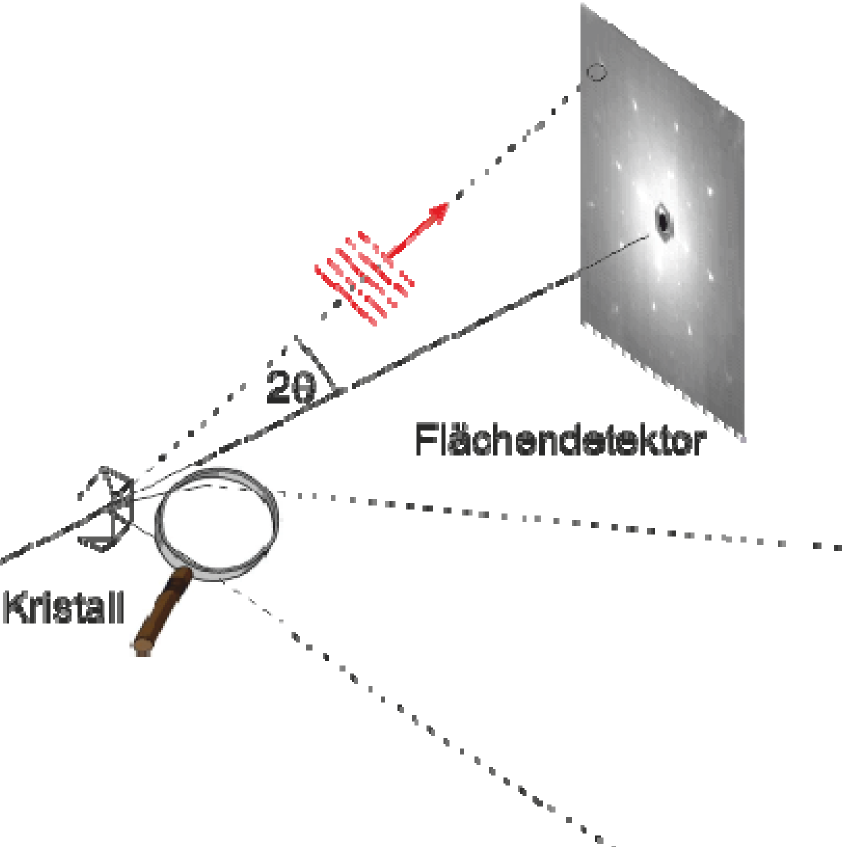
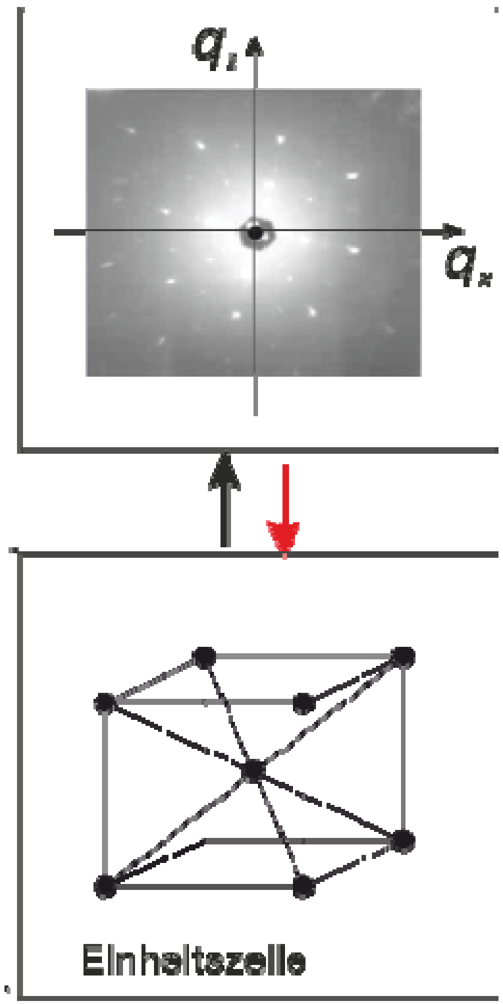

electron density !

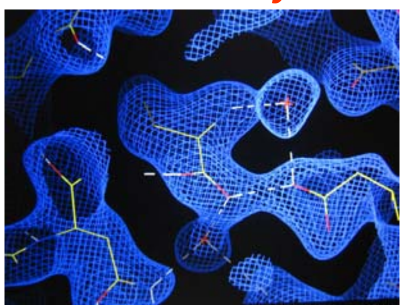

X-ray nobel prizes:
Laue, Bragg, Debey, Perutz&Kendrew, Hodgkin, Watson&Crick,
Deisenhofer, Huber & Michel, Agre, McKinnon,
And many more (> 25 scientists !)

The phase problem

Amplitude ***Phase***

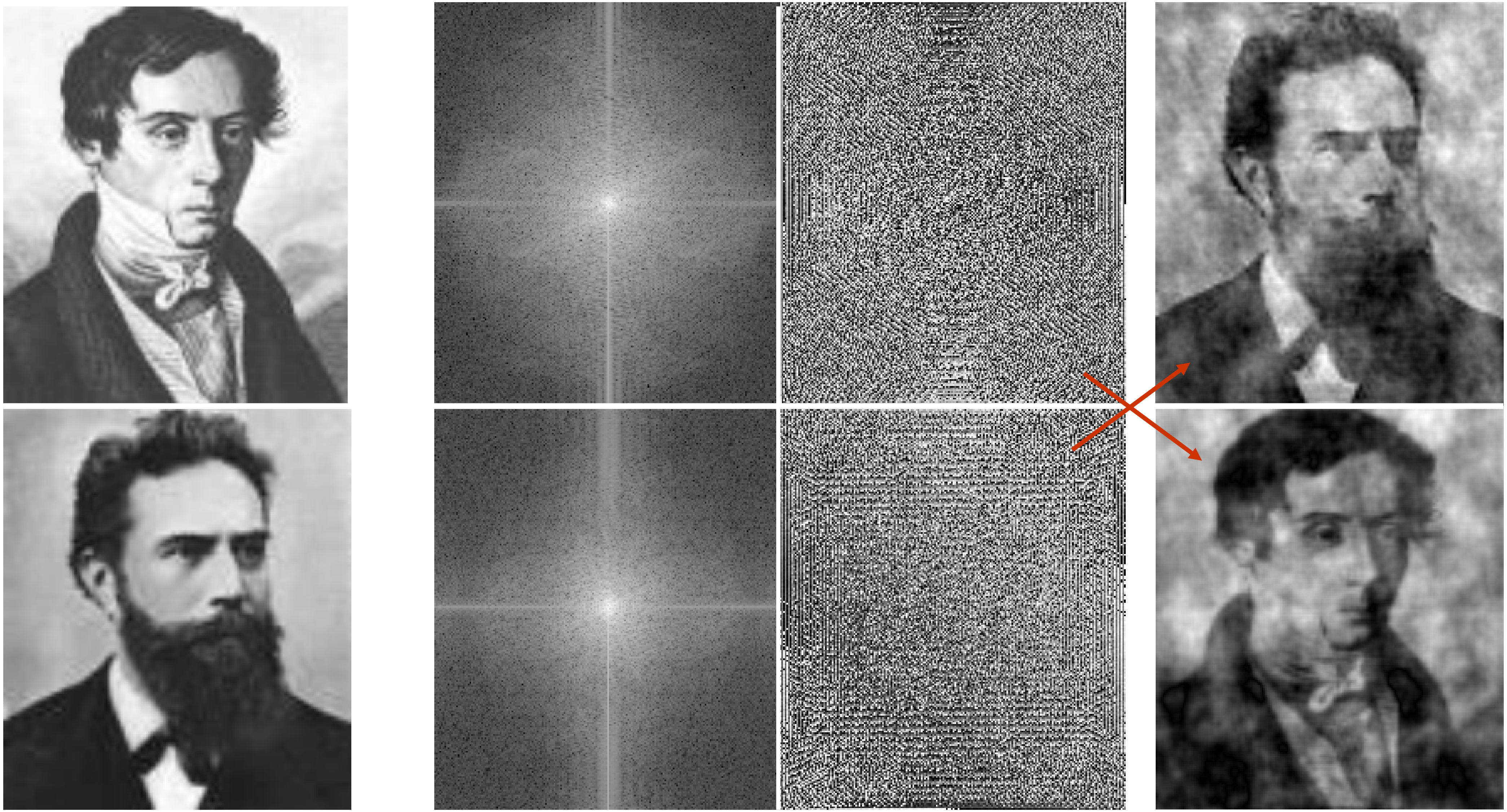

$$\hat{\rho}_{kl} = \frac{1}{\sqrt{N \cdot M}} \sum_{i=0}^{N-1} \sum_{j=0}^{M-1} \rho_{ij}\, e^{-2\pi i\left(\frac{ik}{N}+\frac{jl}{M}\right)}$$

$$\Delta x \approx \frac{\lambda}{2n \sin \alpha}$$

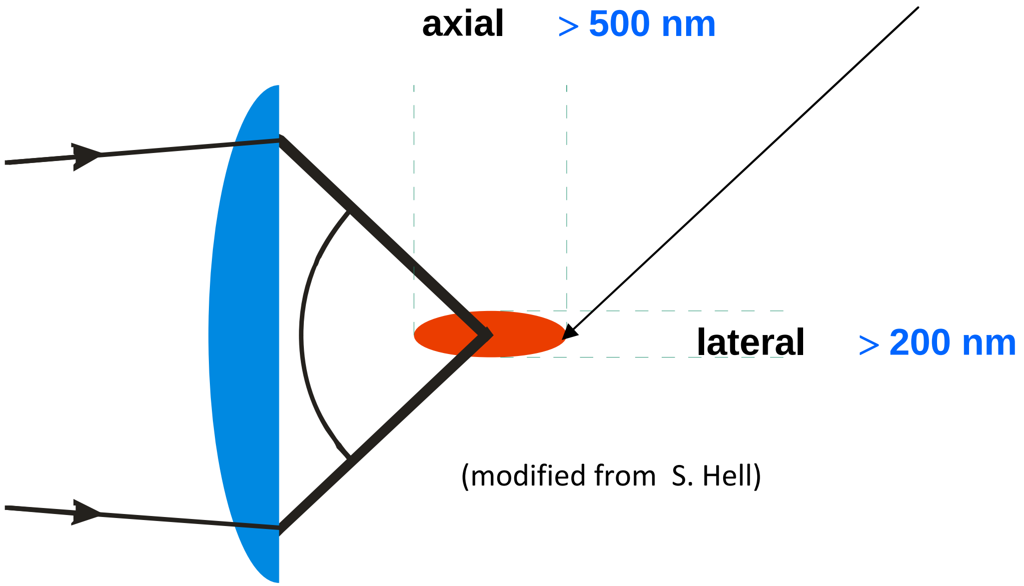

lens / zone plate

Conventional
light microscopy
is limited by diffraction.

Conventional
X-ray microscopy
is limited by diffraction
Structures.

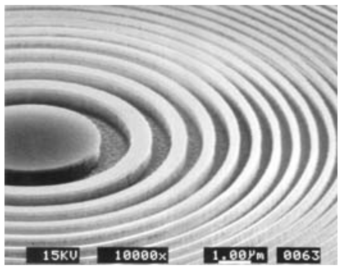

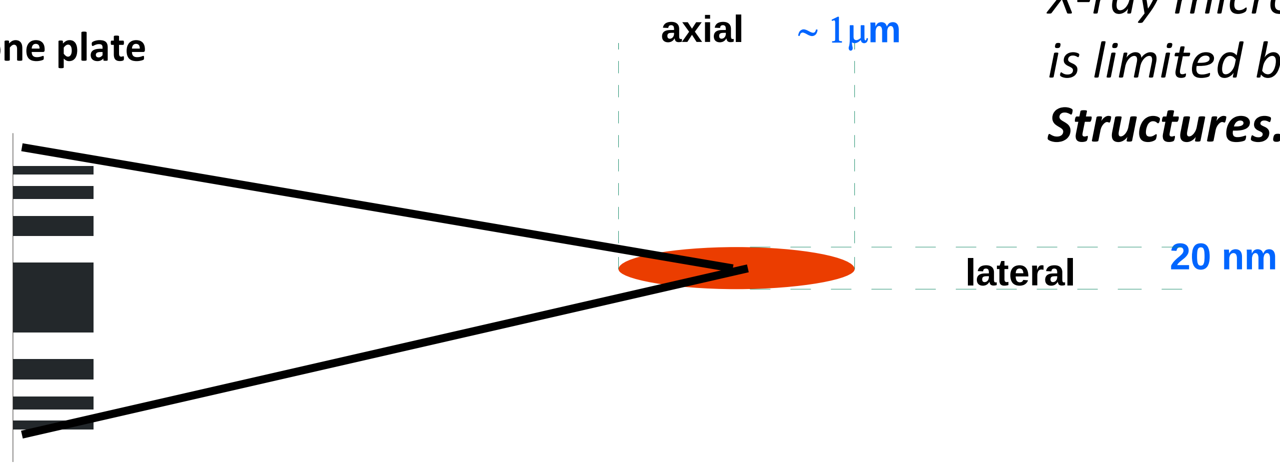

Fresnel Zone Plate (FZP)

„Oversampling“: a strategy to render the problem unique ?

real space $|\mathcal{F}|$ **reciprocal space**

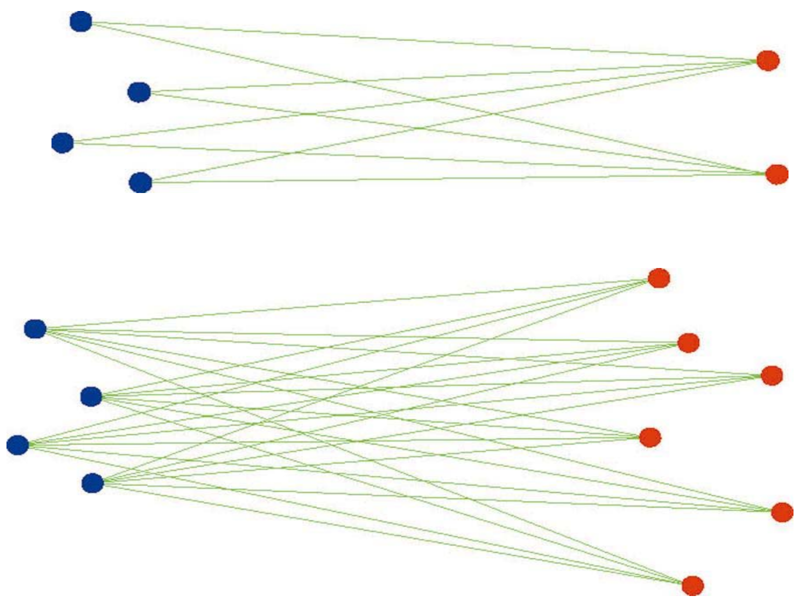

“Oversampling”

Information theory (Shannon) ?
really more information

$$I(q_{kl}) = F(q_{kl})\, F^*(q_{kl}) = \left| \sum_{i}^{N-1} \sum_{j}^{N-1} \rho_{ij}\; e^{-i(q_k x_i + q_l y_i)} \right|^2$$

$$h, k, i, j = 0 \ldots N-1$$

$$F(q) = F^*(-q)$$

J.Miao et al., *J. Opt. Soc. Am.* ’98
J.Fienup, *Appl. Opt.* 21, 2758 (1982)
J.Miao, J. Kirz & D. Sayre, *Acta Cryst*. D 56, 1312 (2000)

„Oversampling“: a strategy to render the problem unique ?

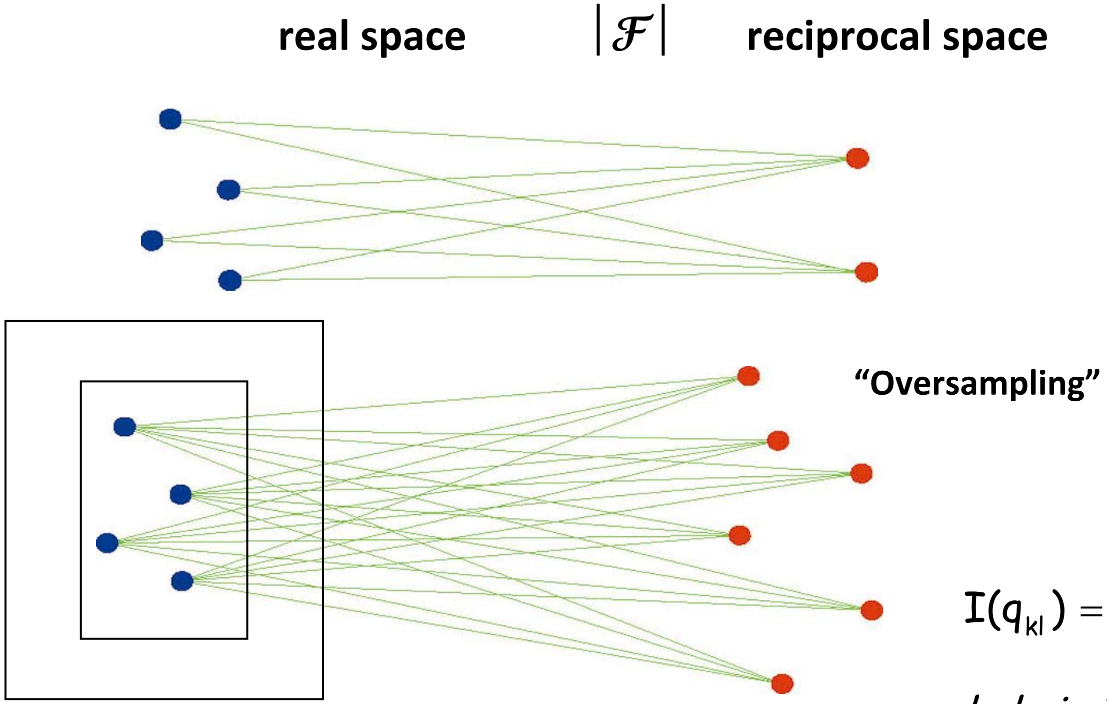

Information theory (Shannon) ?
really more information

$$\text{I}(q_{kl}) = \text{F}(q_{kl})\,\text{F}^*(q_{kl}) = \left| \sum_{i}^{N-1} \sum_{j}^{N-1} \rho_{ij}\; e^{-i(q_k x_i + q_l y_i)} \right|^2$$

$$h,k,i,j = 0 \ldots N-1$$

$$F(q) = F^*(-q)$$

N^2 unknowns r_{ij},
but only $N^2/2$ independent equations

ρ(r) =0 out of support !

If support is half the size of
the field of view in both both dimensions:

N^2 unknowns ρ_{ij},
4 N^2 equations
2 N^2 independent equations

J.Miao et al., *J. Opt. Soc. Am.* ’98
J.Fienup, *Appl. Opt.* 21, 2758 (1982)
J.Miao, J. Kirz & D. Sayre, *Acta Cryst*. D 56, 1312 (2000)

how to solve the nonlinear set of equations: iterative algorithms

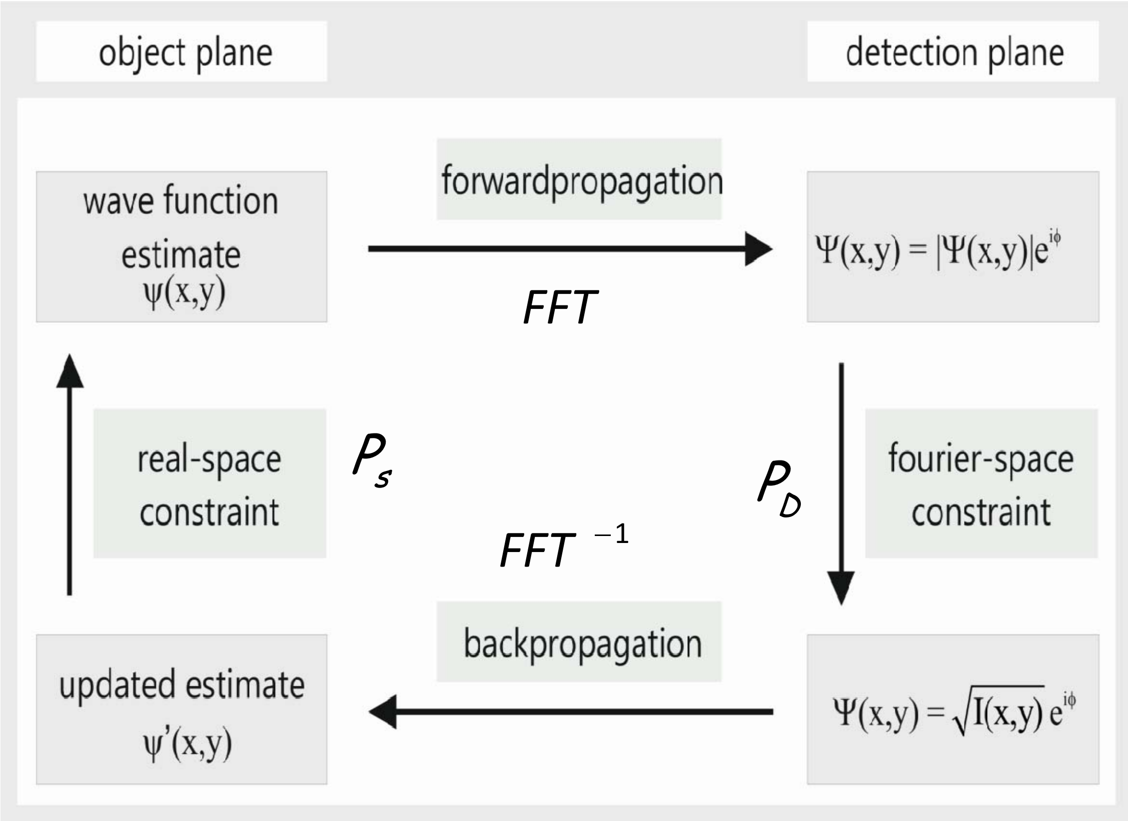

$$\rho_{i+1}(r) = \begin{cases} \rho_i^{'}(r) & r \in S \cap \rho_i^{'}(r) > 0 \\ \rho_i(r) - \beta\, \rho_i^{'}(r) & r \notin S \cup \rho_i^{'} \leq 0 \end{cases}$$

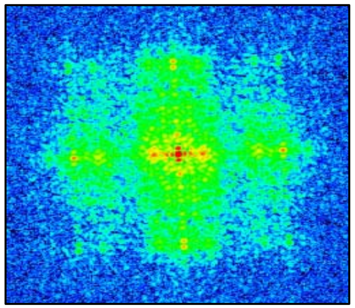

coherent scattering patte

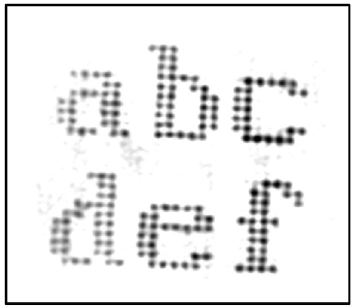

reconstructed image

J. Miao et al., Nature ***400****, 342 (1999)*

Ptychography: using the overlap constraint

$$\Psi(\mathbf{r}) = P(\mathbf{r} + (0,0,d)) \cdot O(\mathbf{r}) \qquad |\mathcal{F}(\Psi)|^2 = |\mathcal{F}(P_d) \times \mathcal{F}(O)|^2$$

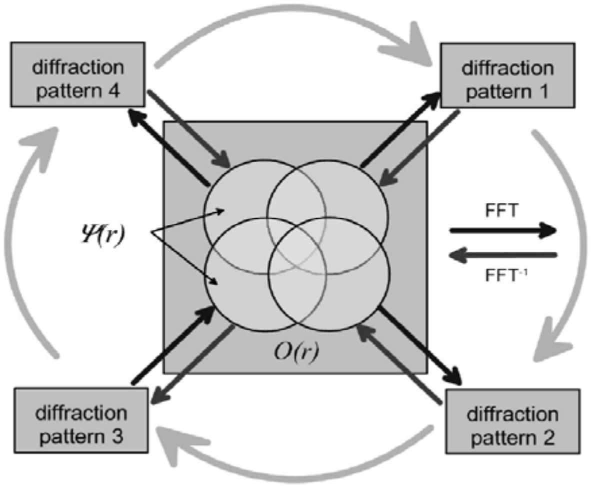

Rodenburg *et al. PRL* **98**, 034801 (2007)

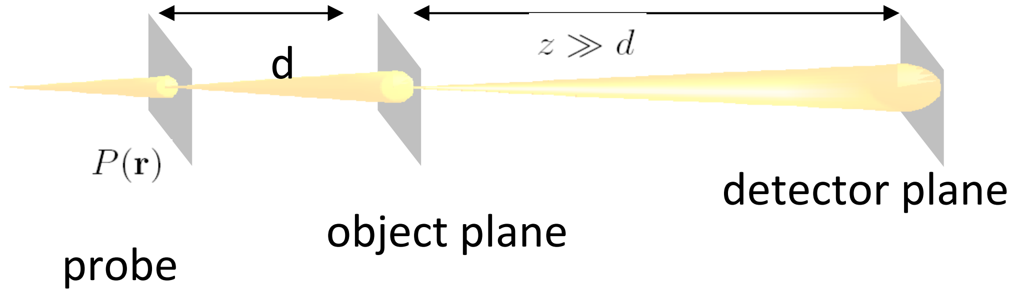

ptychographic reconstruction with x-rays:
Rodenburg *et al.* PRL (2007)

simultaneous reconstruction of illumination field:
Thibault *et al.* Science (2008)
Guizar-Sicairos, Fienup, Optics Express (2008)

application to biological cells:
Klaus Giewekemeyer *et al.*, PNAS (2010)

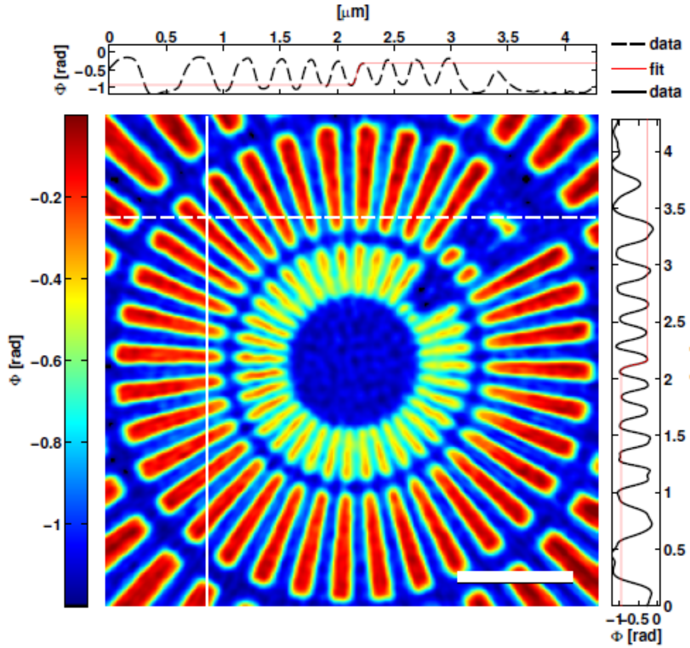

(a)

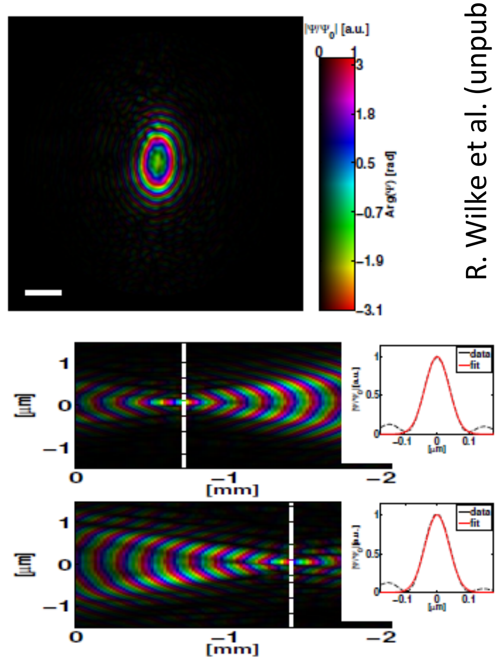

(b)

R. Wilke et al. (unpublished)

scanning and diffraction

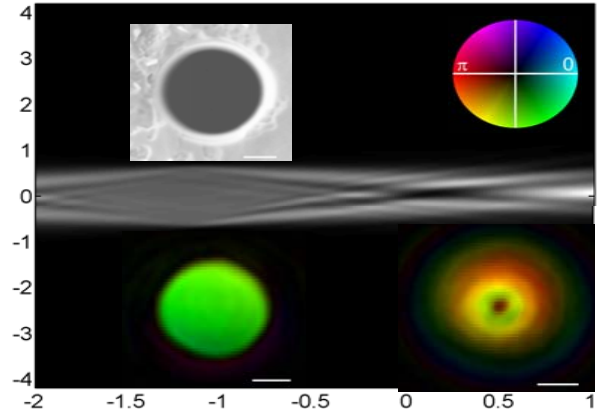

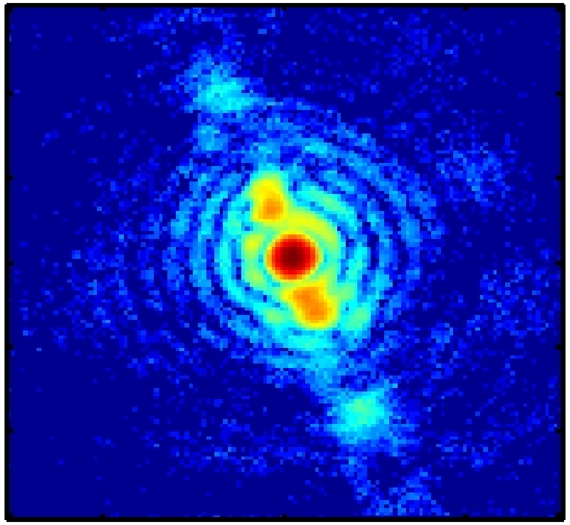

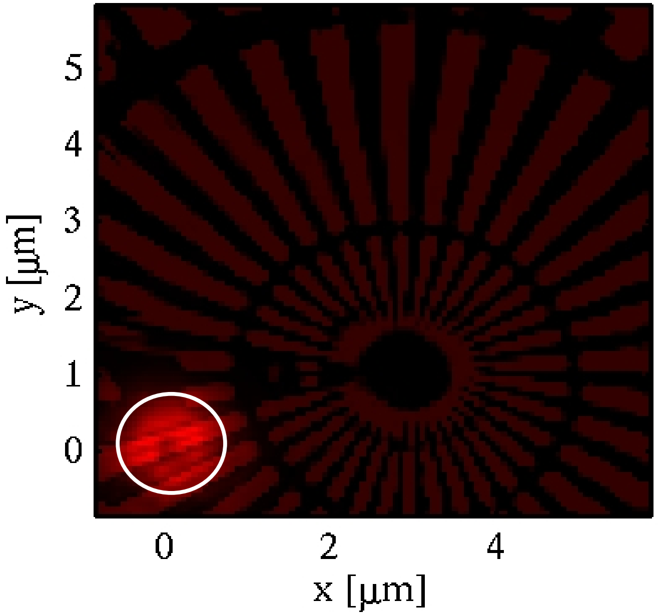

Maximum spacial frequency given by detector size and distance (Pilatus pixel det.)

15/µm (d = 67nm), possible, but noise issues (Poissonian noise)!

Giewekemeyer et al, PNAS 2010

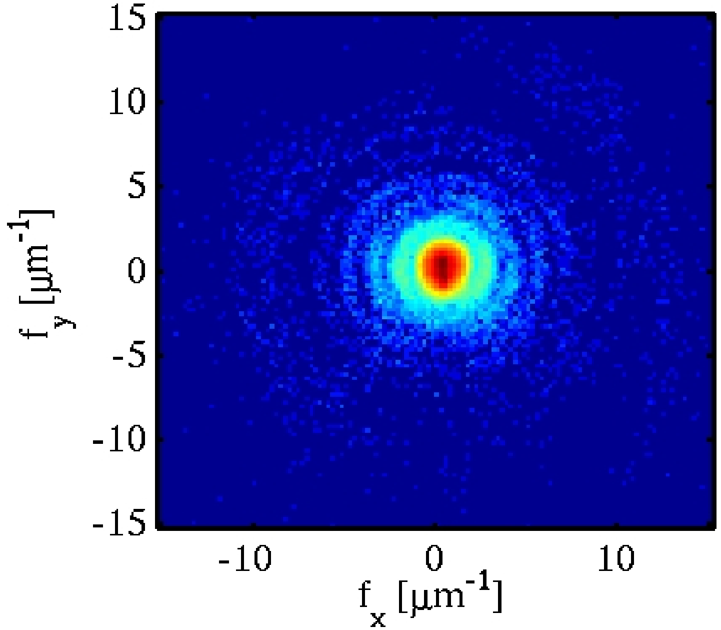

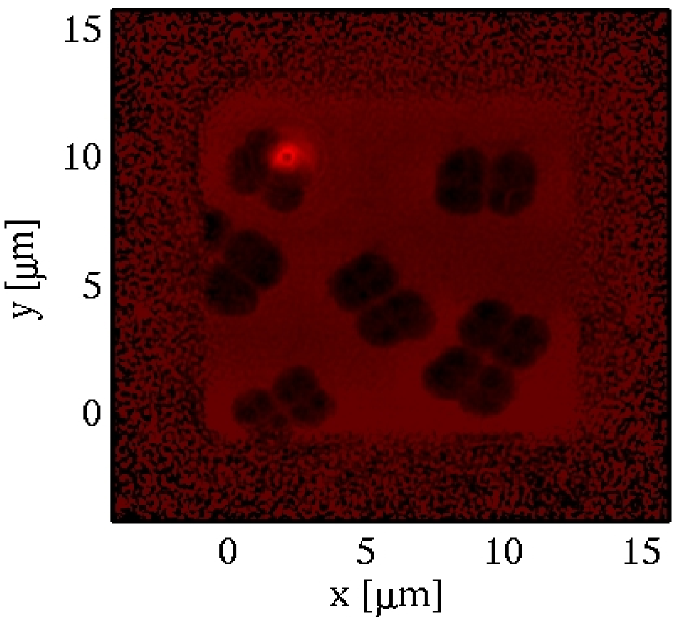

Giewekemeyer et al, PNAS 2010

DNA packing in nucleoids: *Deinococcus Radiodurans*

- **Among most radiationresistant organisms on earth, can survive 15 kGy of ionizing radiation**
- **Very effective DNA repair mechanism, DNA packing debated**

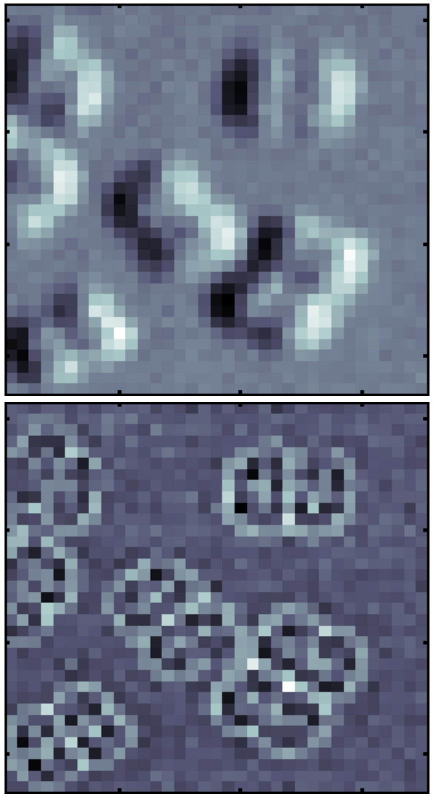

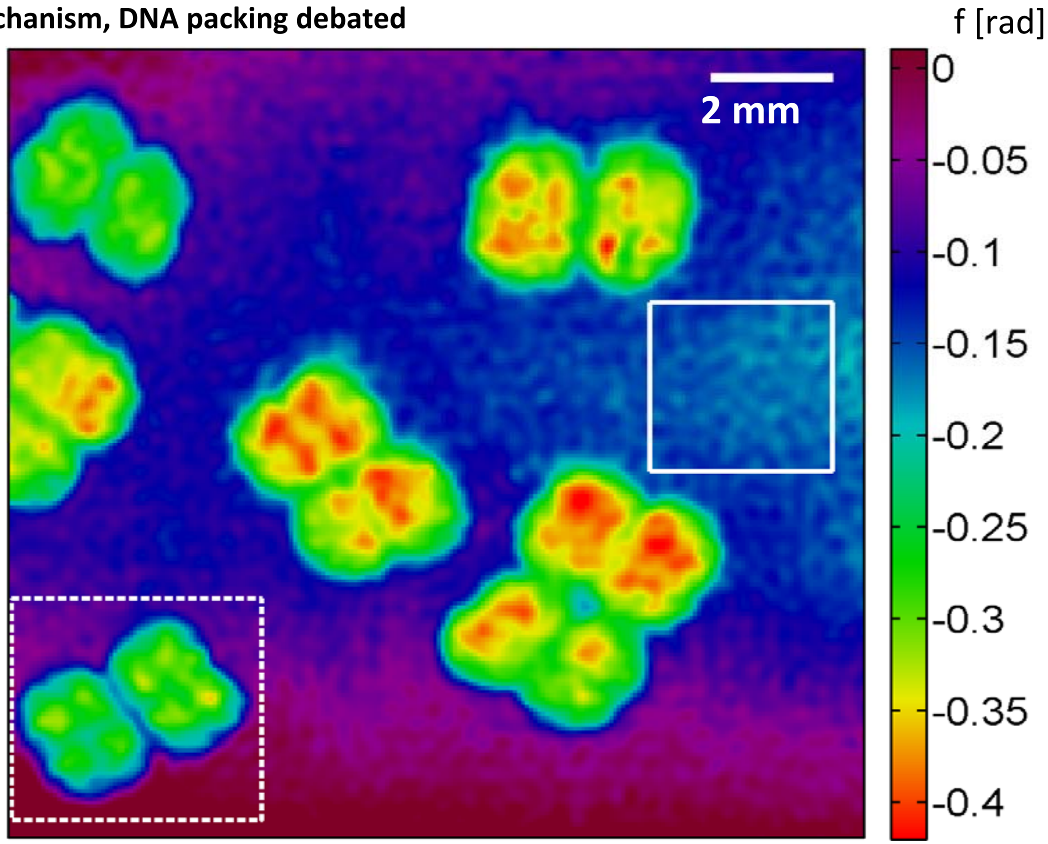

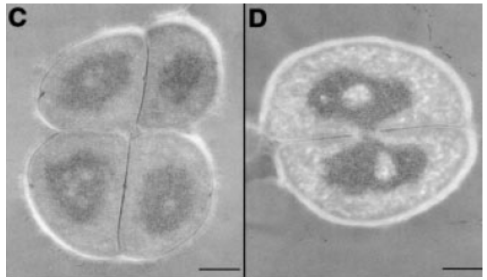

TEM-slices, Os-stained chromatin
Levin-Zaidman, Science (2003)

Left: Scanning X-ray Microscopy
DPC / dark field

Right: super-resolution by phasing the coherent diffraction pattern

2x3 μm size, tetrad morphology
4 identical copies of the genome

- Freeze-dried, unstained and unsliced cells
- Overall phase shift of single cell 0.25-0.3 rad (< 10% p), consistent with simulations
- 2500 iterations of SXDM algorithm, averaged over each 5th iterate, starting at 2000

Giewekemeyer *et al.*, PNAS (2010)

PHYSICAL REVIEW LETTERS

Chemical Contrast in Soft X-Ray Ptychography

Mike Beckers,[1,*] Tobias Senkbeil,[1] Thomas Gorniak,[1] Michael Reese,[2] Klaus Gieweker…
Tim Salditt,[3] and Axel Rosenhahn[1,5,†]

Soft x-rays (water window):
Absorption and phase
Carbon K-edge
-> chemical contrast

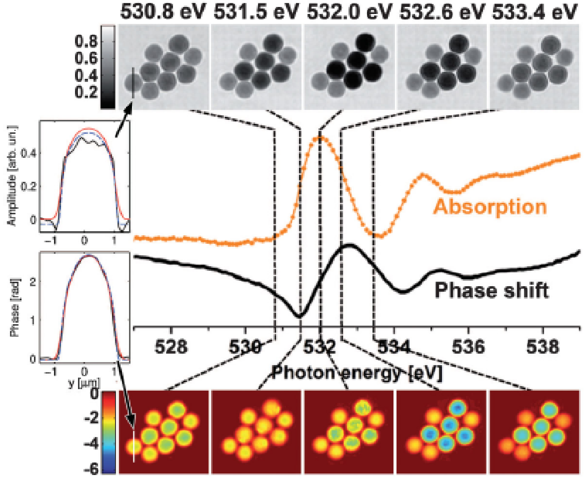

6 FIG. 2 (color). Reconstructions of amplitude and unwrapped phase (in radians) of five ptychographic data sets recorded at different energies around the measured C = O absorption peak of PMMA. The sample, a mixture of five PMMA beads and four SiO_2 beads each 2 μm in size, shows absorption and phase shift

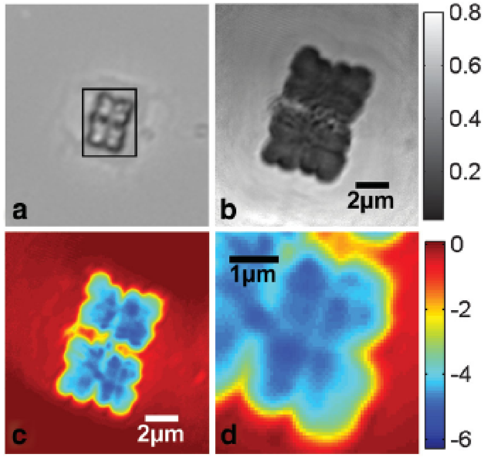

FIG. 3 (color). *D. radiodurans* cells. (a) Bright field microscopy image of a part of the specimen. Marked is the area of the ptychographic scan used for reconstruction. (b) Reconstructed amplitude of the cells. (c) Unwrapped phase shift of the cells and (d) detailed view.

Hard x-rays :
Absorption neglegible
large penetration and focal depth
-> tomography

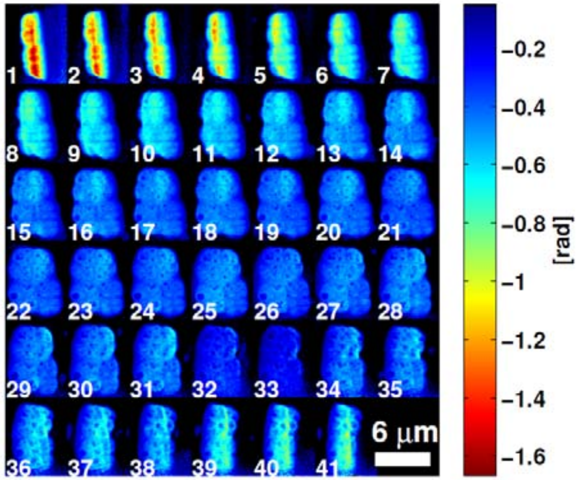

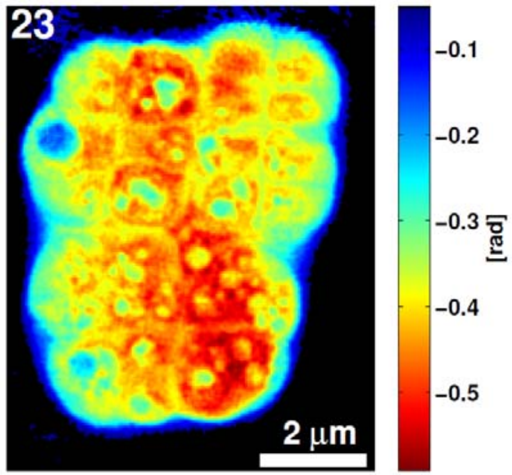

R. Wilke et al. (unpublished)

illumination function: ***plane wave, curved, structured,*** ***unknown ?***

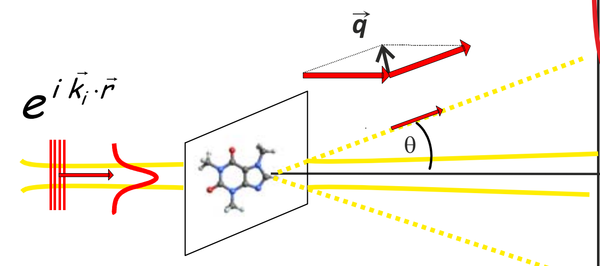

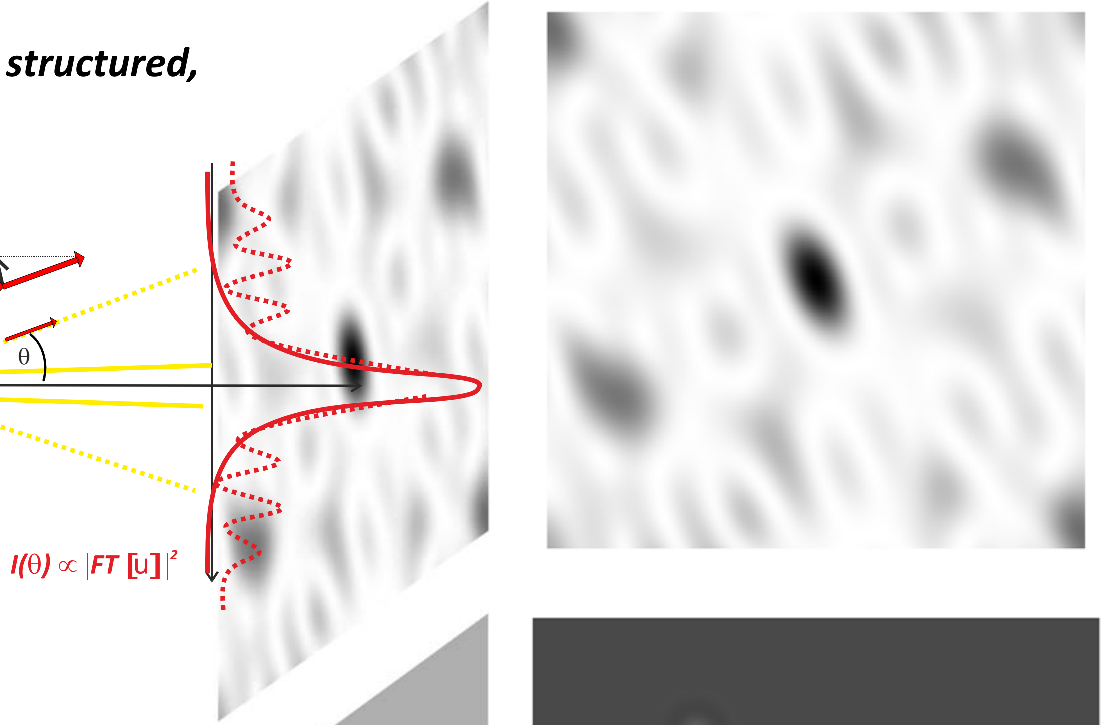

$$u(x,y) = u_0(x,y)\ \tau(x,y)$$

$$\left|FT[u]\right|^2 = \left|FT[u_0]\otimes FT[\tau]\right|^2$$

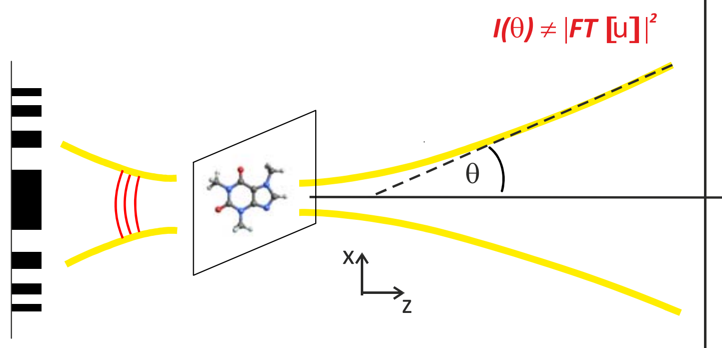

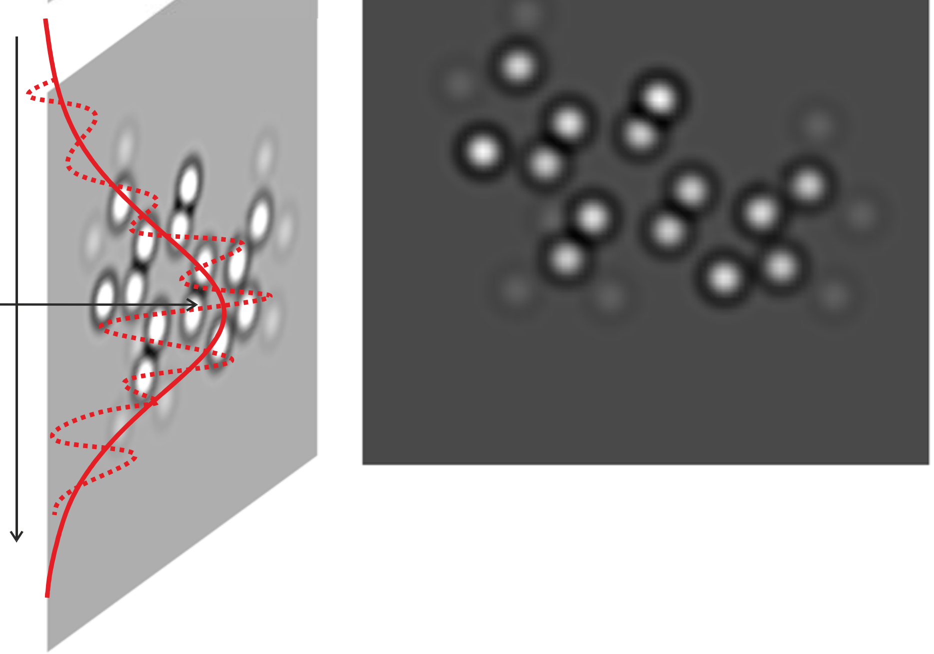

- projection approximation: multiply illumination u_0 and object τ
- measured intensity: convolution of illumination and object

Far-field and near-field diffraction patterns !

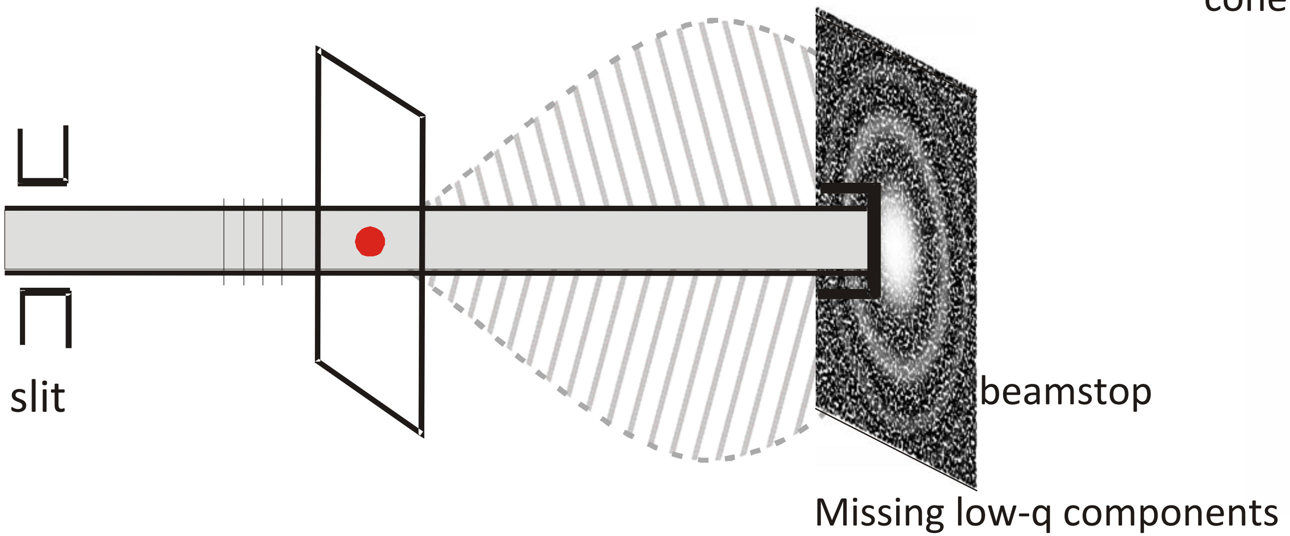

coherent farfield diffraction pattern

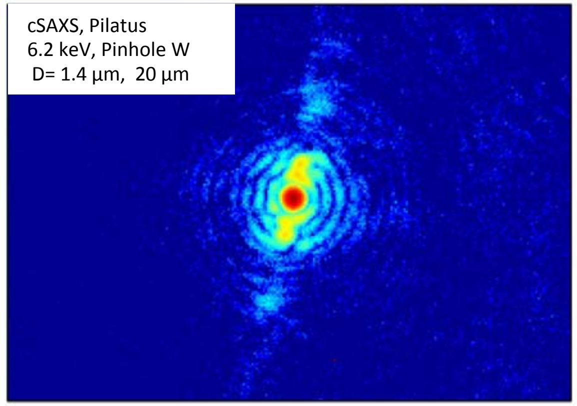

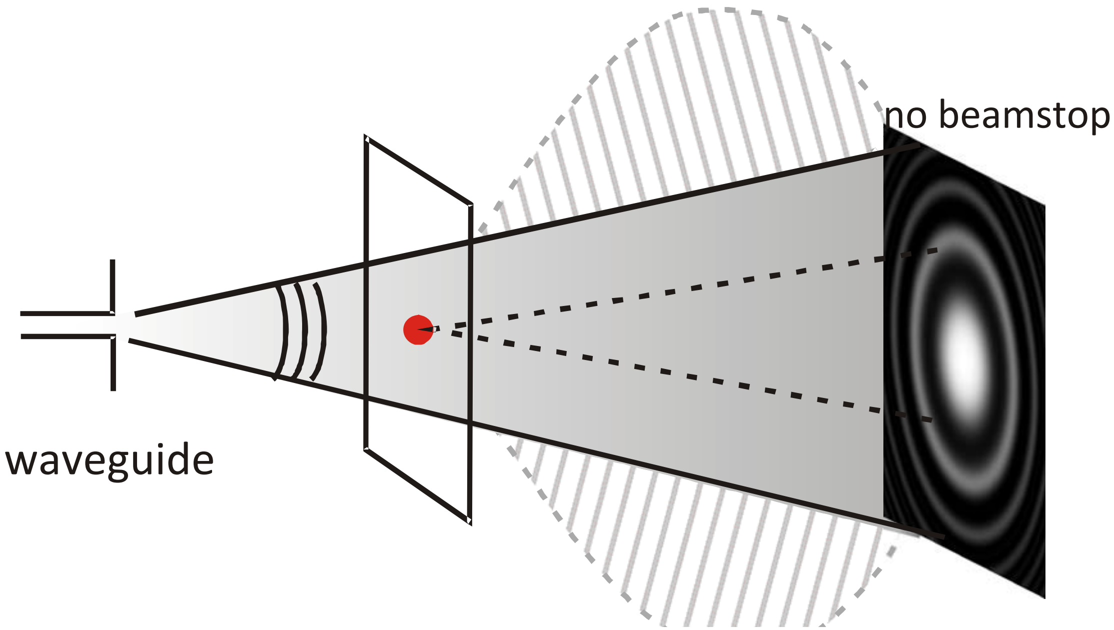

Fresnel diffraction pattern

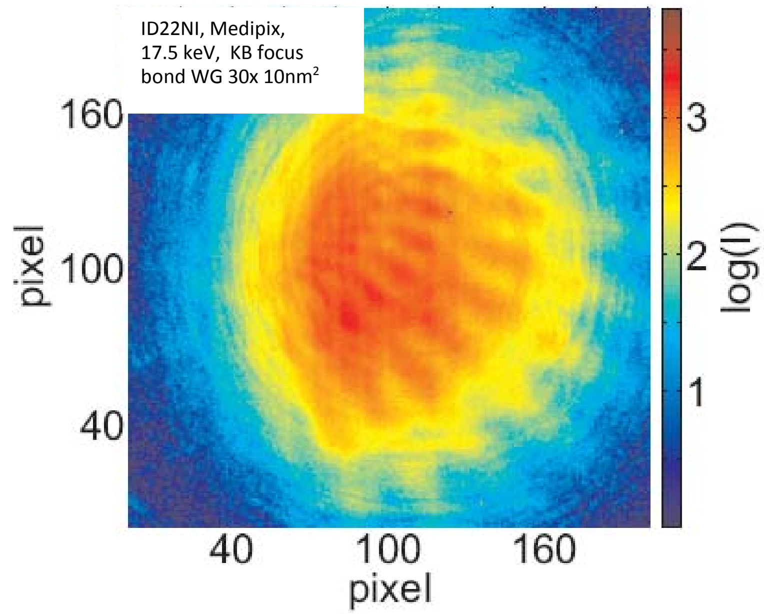

Fresnel scaling theorem:

an equivalence between parallel and point source illumination

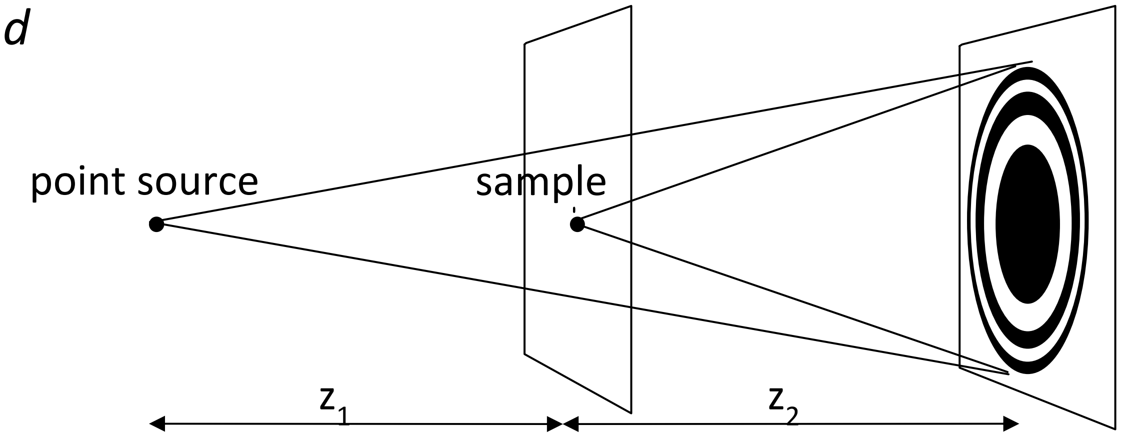

hologram recorded with the point source corresponds to a hologram recorded with a plane wave at an effective defocusing distance

$$z_{eff} = \frac{z_1 z_2}{z_1 + z_2}$$

magnified by

$$M = \frac{z_1 + z_2}{z_1}$$

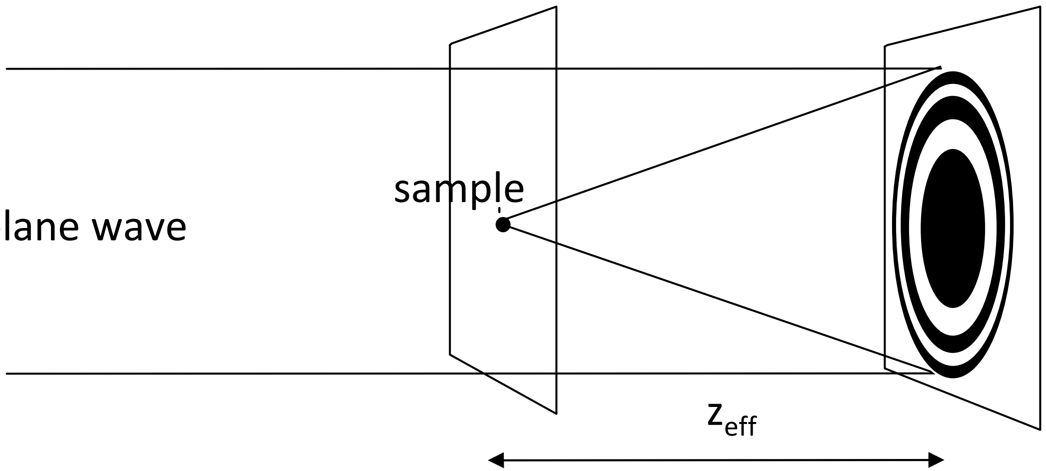

→ magnification allows for a spatial resolution below detector pixel size!

→ plane wave setup used for simulations and reconstruction

Imaging formation: Fresnel diffraction integrals

$$\psi(x',y',z) = \frac{1}{i\lambda}\int_{-\infty}^{\infty}\int_{-\infty}^{\infty}\psi(x,y,0)\frac{1}{r}\exp(ikr)\frac{1+\cos(\vec{n}\cdot\vec{r})}{2}dxdy \qquad \psi(x,y,0) = \psi_0\,\tau(x,y)$$

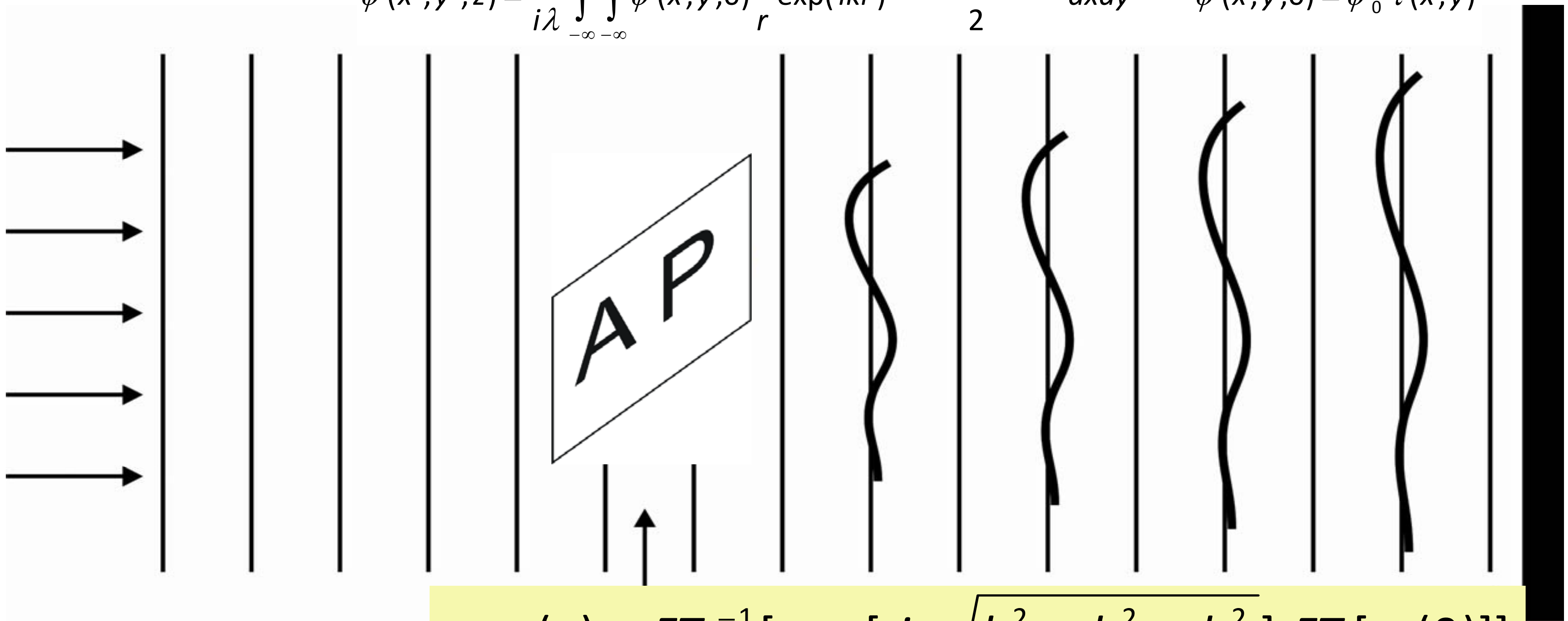

$$\psi(z) = FT^{-1}[\exp[iz\sqrt{k^2 - k_x^2 - k_y^2}]\,FT[\psi(0)]]$$

object with complex transmission function $\tau(x,y)$

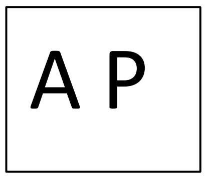

Absorption Phase

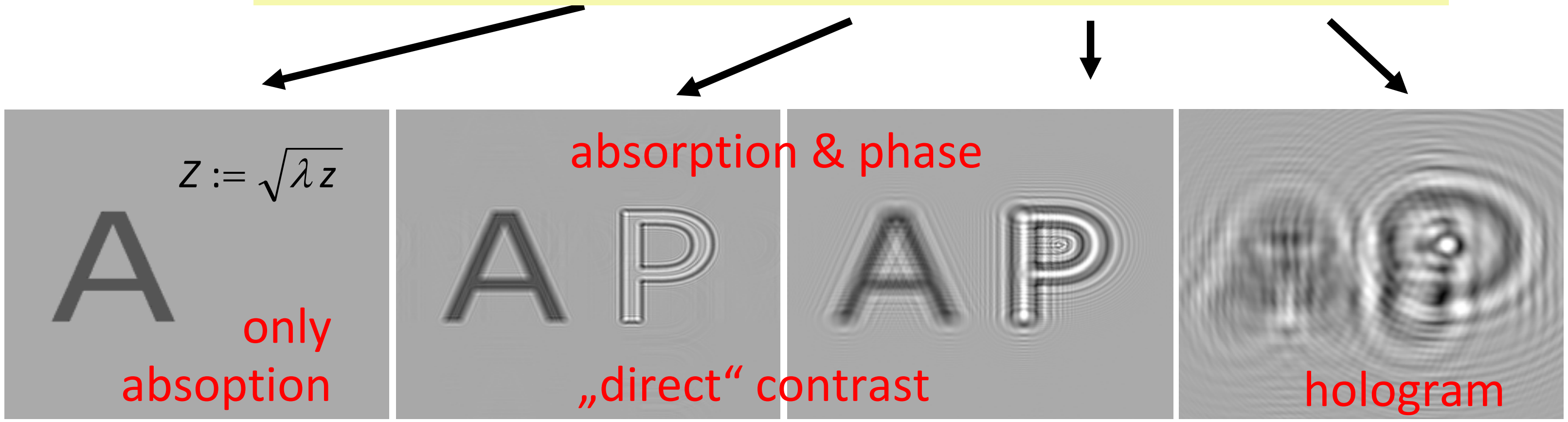

transformation from spherical to parallel beam, $z \to z_{eff}$, M magnified coordinate system

$$I(x,y) = |D_{z_{\text{eff}}}[\psi_{\text{in}}\chi(x,y)]|^2 \simeq |\psi_{\text{in}} D_{z_{\text{eff}}}[\chi(x,y)]|^2$$

normalisation of the measured intensity I by empty beam

$$\bar{I}(x,y) \simeq |\psi_{\text{in}} D_{z_{\text{eff}}}[\chi(x,y)]|^2 / |\psi_{\text{in}}|^2 = |D_{z_{\text{eff}}}[\chi(x,y)]|^2.$$

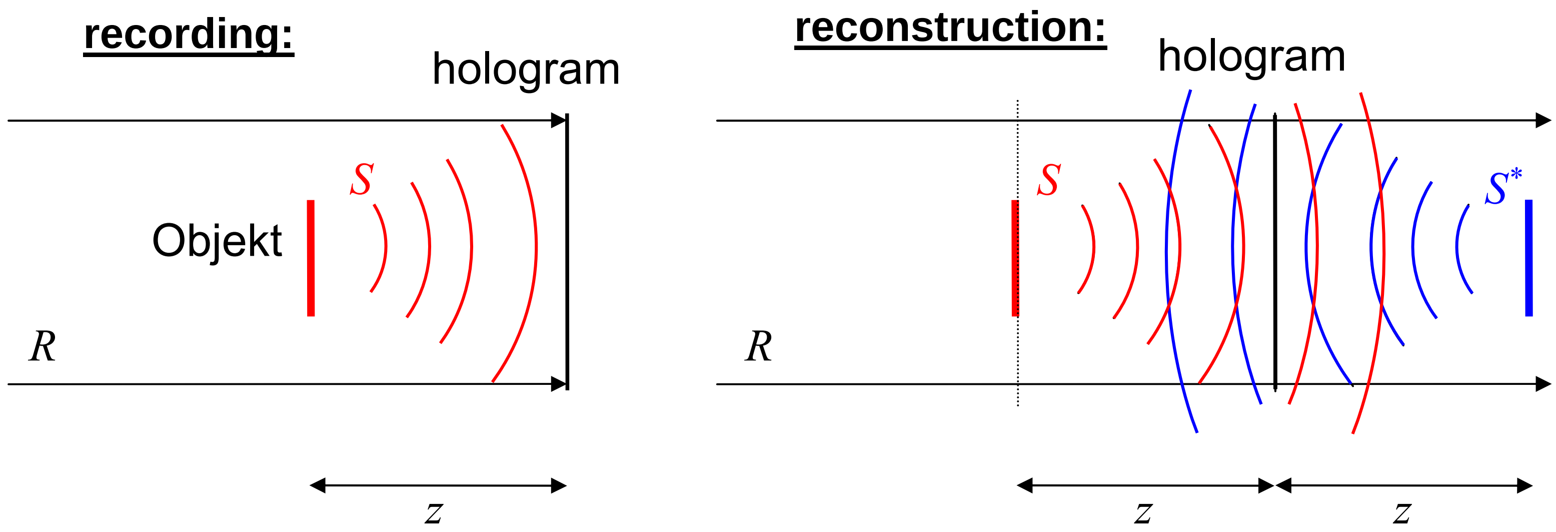

reference beam

signal

conjugated wave „twin image“

$$\chi(x,y) = 1 + \tau(x,y)$$

$$\tau \xrightarrow{D_z} \tilde{\tau} = D_z[\tau]$$

$$I(x,y) \propto |1+\tilde{\tau}|^2 = 1 + \tilde{\tau} + \tilde{\tau}^* + |\tilde{\tau}|^2$$

$$\tau_{recon} = D_{-z}[1 + \tilde{\tau} + \tilde{\tau}^* + |\tilde{\tau}|^2] = 1 + \tau + \tau^* + D_{-z}\left[|\tilde{\tau}|^2\right]$$

Waveguide based propagation imaging
schematic setup

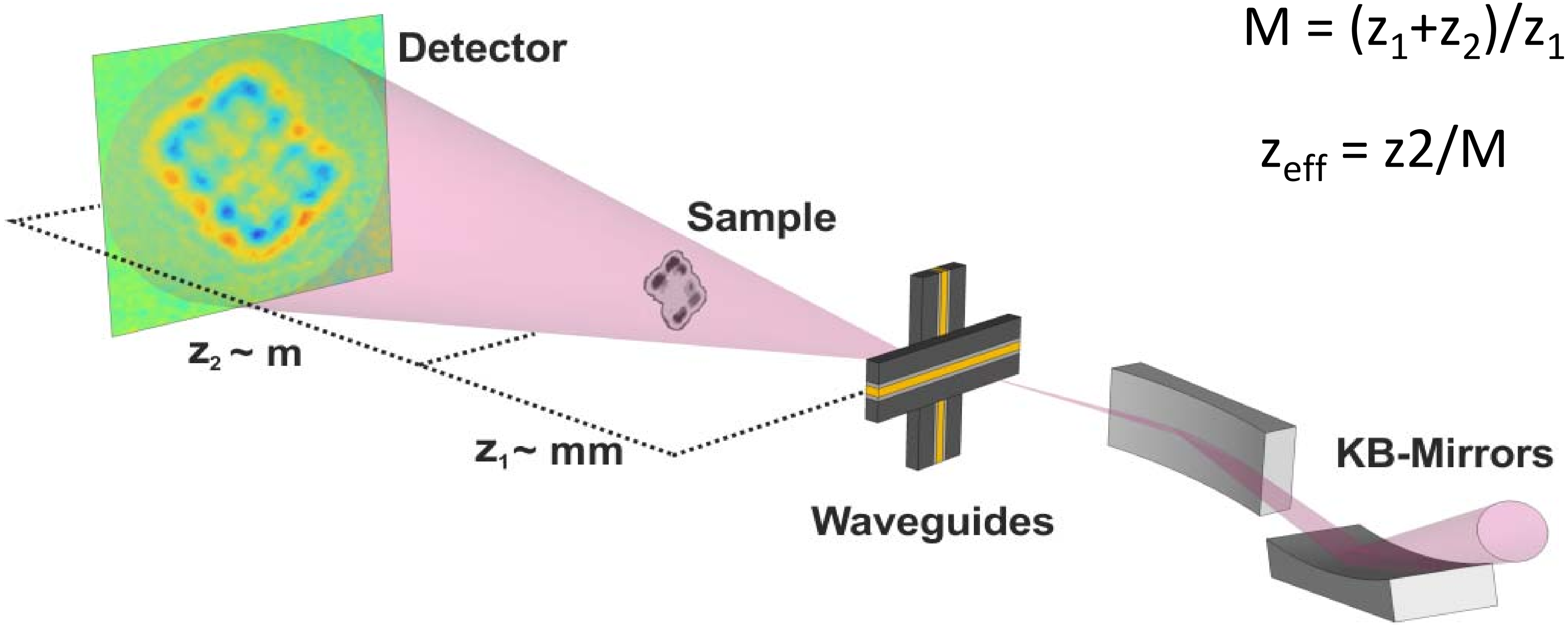

$M = (z_1+z_2)/z_1$

$z_{eff} = z2/M$

1. Homogeneuos signal level in detection plane
2. High dose efficiency
3. Less scanning overhead for tomography (full field)

M. Bartels et al. , unpublished , 2011

Waveguide based propagation imaging

setup – P10 at PETRA III

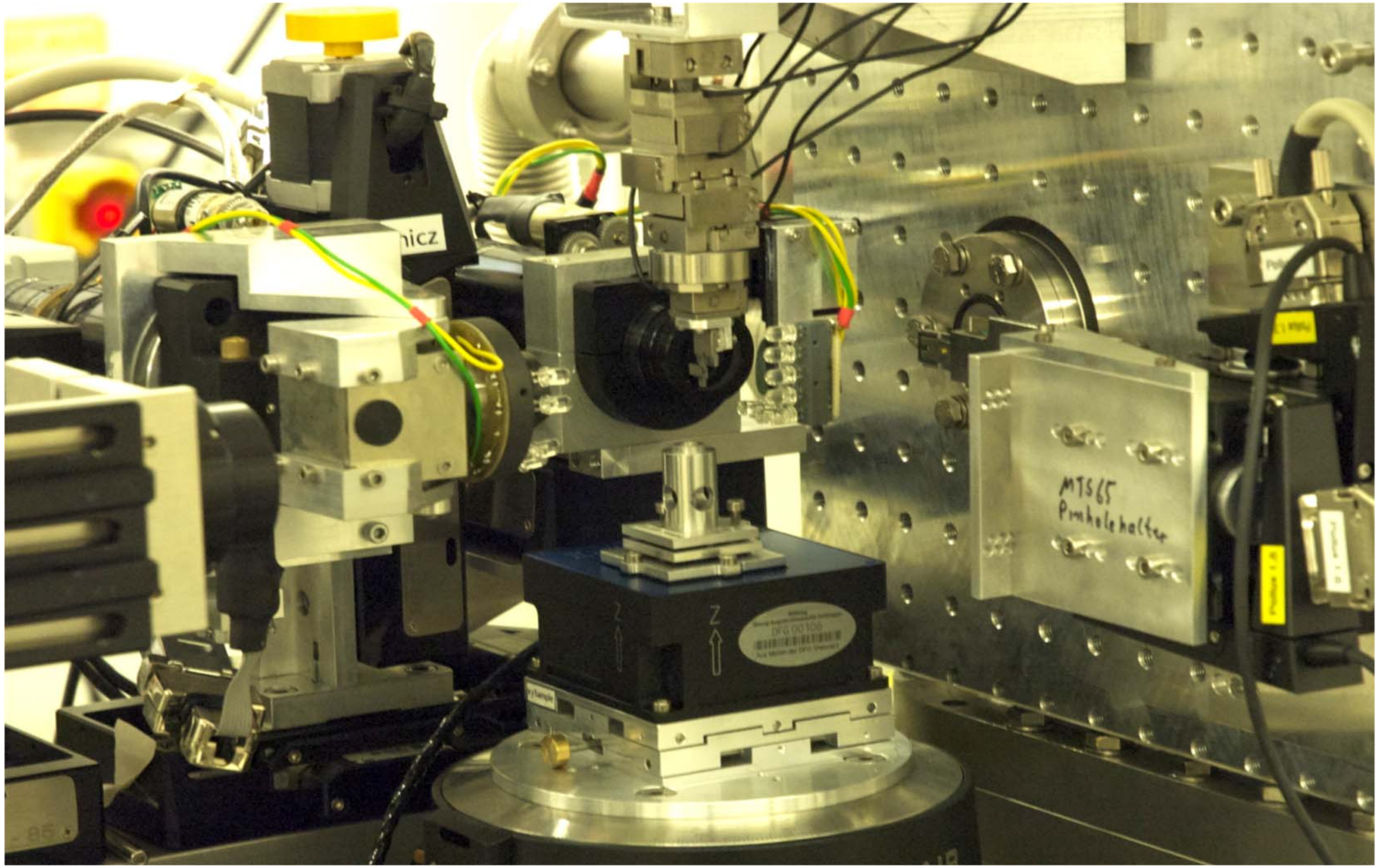

Kalbfleisch et al. , AIP Conf. Proc., 2011

KB mirrors

mirror –precision polishing and metrology

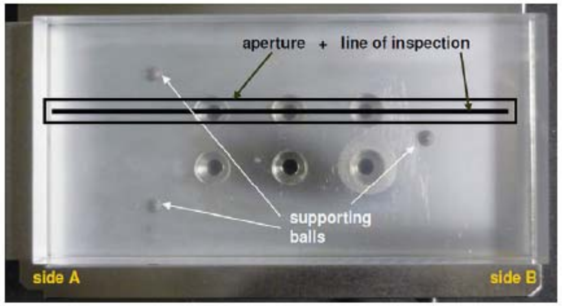

Fig. 3. Hard X-ray focussing mirror for the holography end-station of beamline P10 at PETRA-III at the alignment set with three steel balls. The 10 mm thick substrate was finished on a 10 mm × 5 mm long aperture section by EEM-finishing technology.

Table 1
Shape parameter of an elliptical cylinder mirror, for hard X-ray focussing at PETRA-III, as measured using BESSY-NOM and a Micromap Promap interference microscope (using magnifications 2.5 ×, 20 × and 50 ×).

Parameter of ellipse	Specification	Measurement results
Source distance r (mm)	85 500	85 500
Focus distance r' (mm)	200	200
Incidence angle θ (mrad)	4.0	4.0499
Mirror pole x_m (mm)	Not defined	42 648.2
Residual slope error		0.13 μrad rms
Residual figure error	3 nm pv	1.0 nm rms/3.1 nm pv
Roughness	≤0.15 nm rms	S_q=0.135–0.164 nm rms (2.5 ×) =0.107–0.122 nm rms (20 ×) =0.101–0.122 nm rms (50 ×) S_a=0.106–0.126 nm rms (2.5 ×) =0.082–0.096 nm rms (20 ×) =0.079–0.093 nm rms (50 ×)

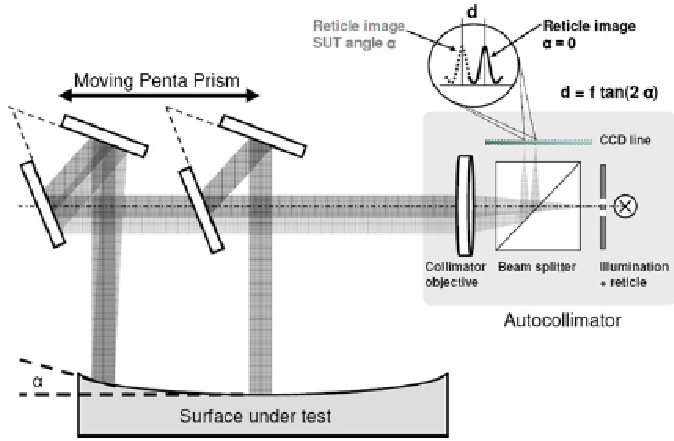

Fig. 1. Principal set-up of a mirror based moving penta-prism slope measuring profiler as realized for BESSY-NOM.

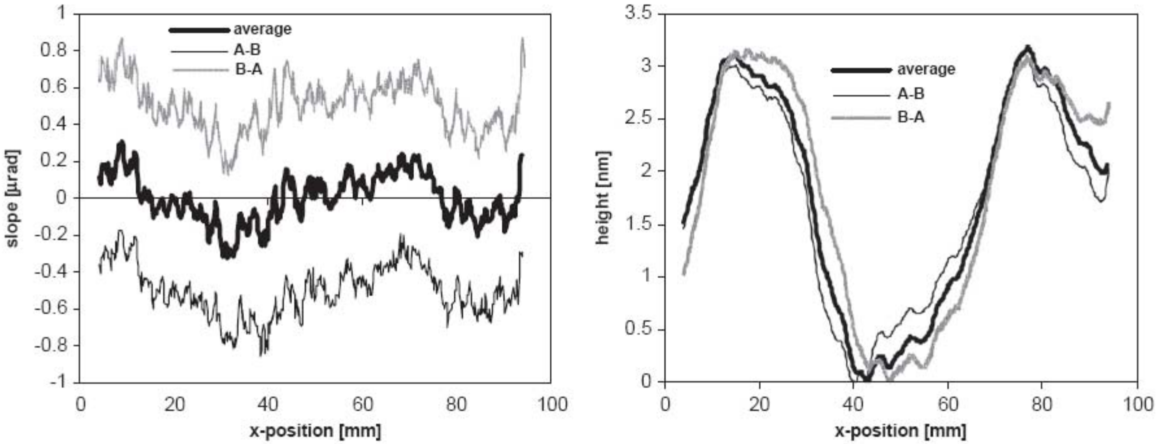

Fig. 4. Hard X-ray focussing mirror for the holography end-station of beamline P10 at PETRA-III. Left—profile of residual slope measured at two different alignment conditions from side A to B and after a 180° rotation from side B to A. For better visualization a shift of 0.2 μrad was added to the profiles. Right—the corresponding profiles of residual height, gained by integration of the slope data.

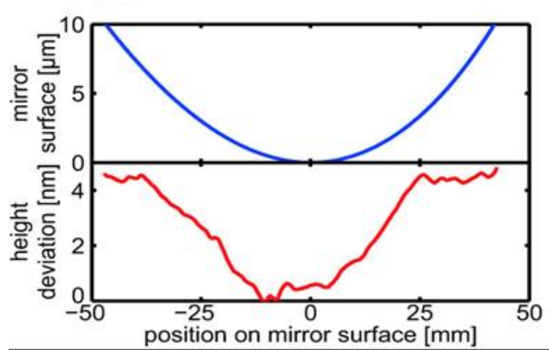

Elastic emission machining and Interferometry (Yamauchi group, Osaka University
Commercialized by JTEC Corp, Osaka
Metrology: F. Siewert et al., NIM A 2011

measured intensity distribution compared to simulation

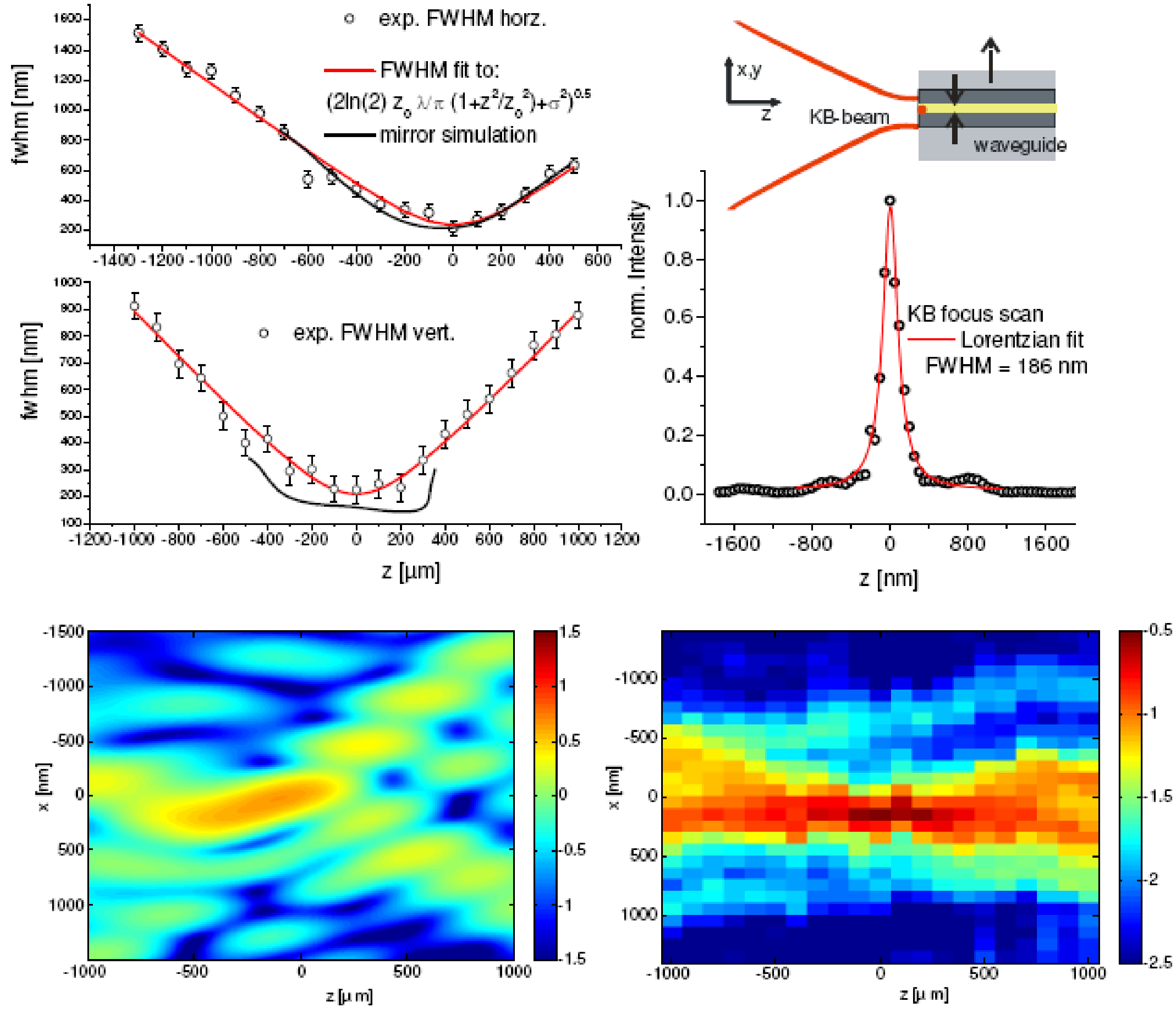

T. Salditt et al. Opt. Express 2011

KB mirror system

height profile JTEC mirror

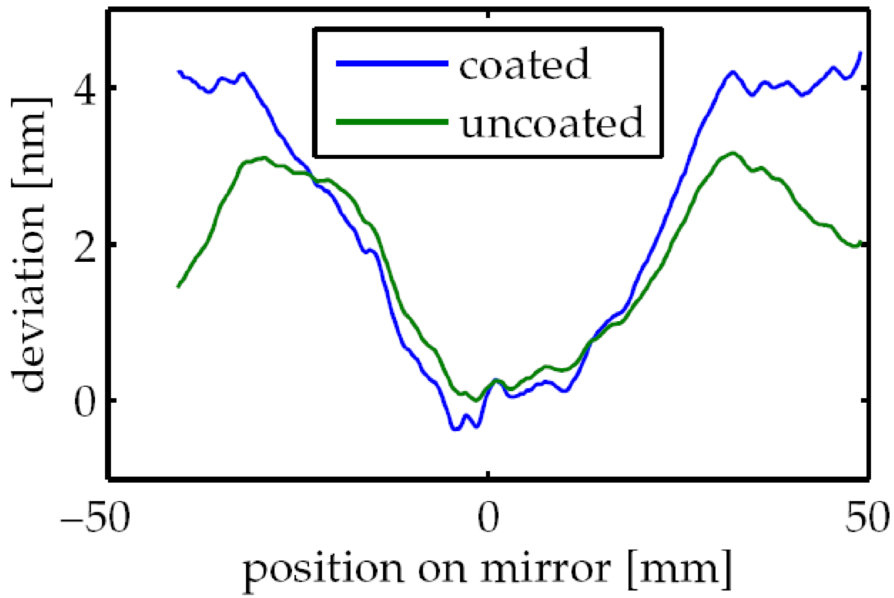

height profile WINLIGHT mirror

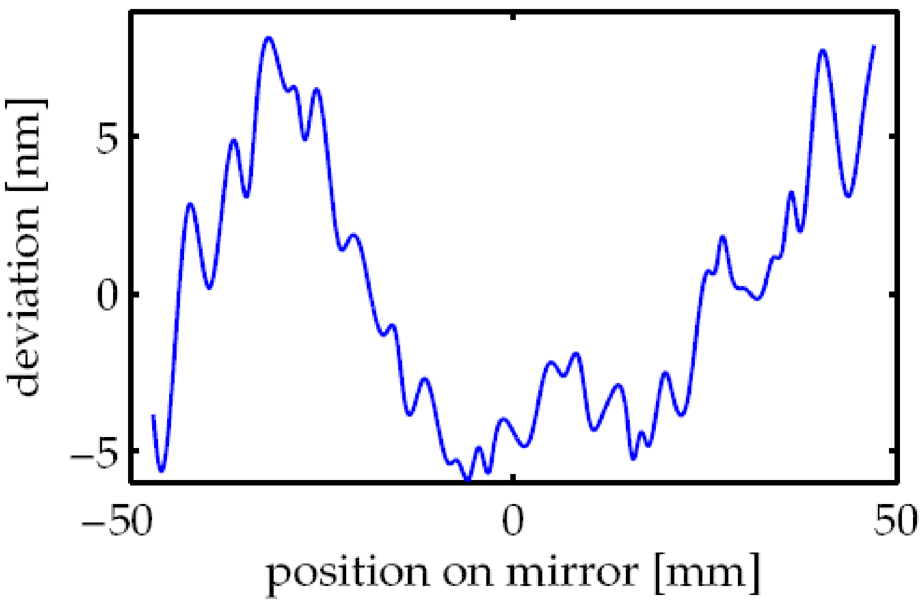

Simulated farfield pattern
based on measured height data

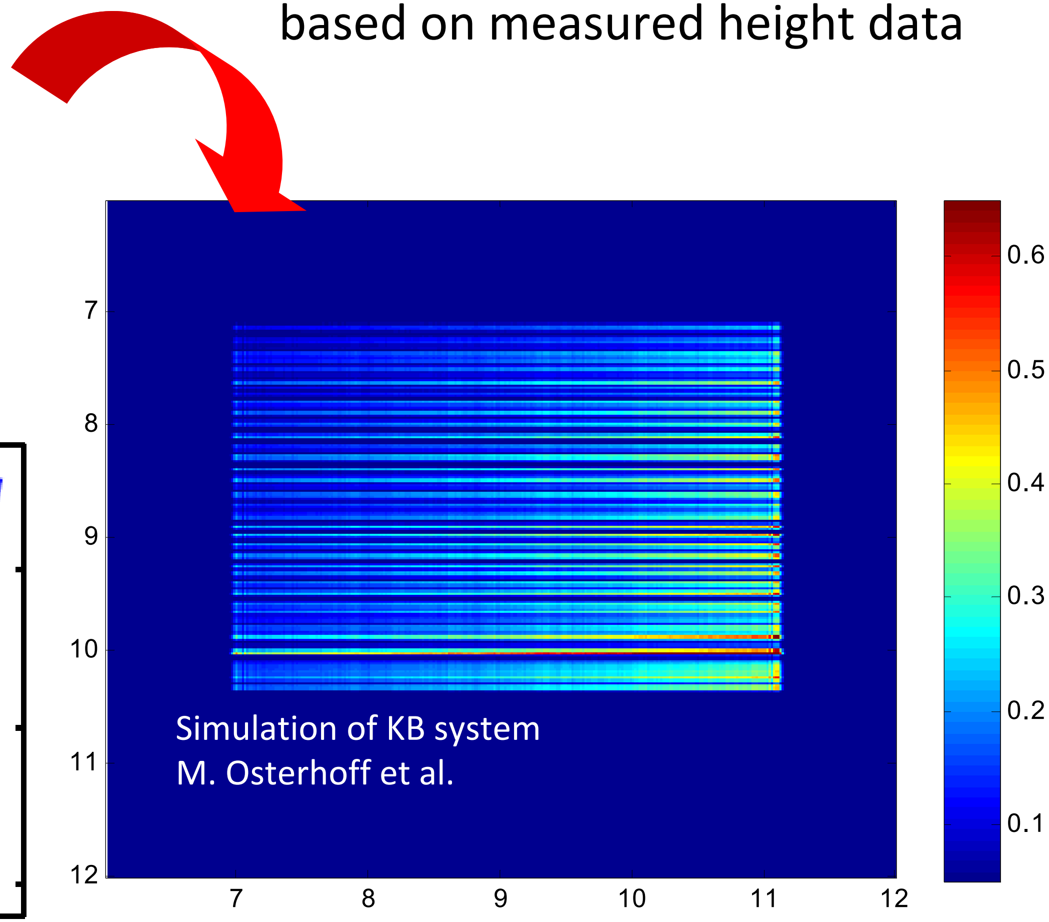

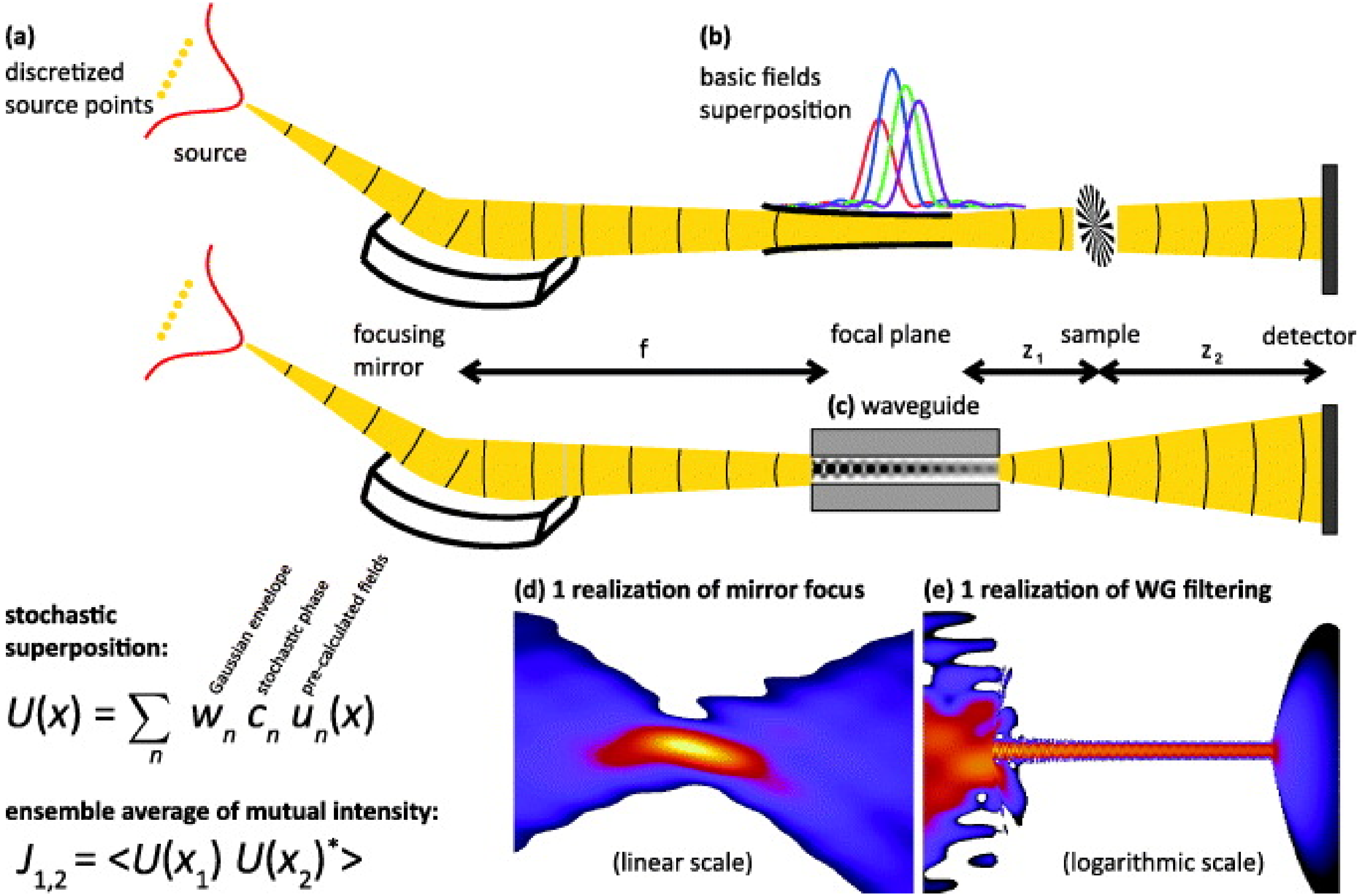

Osterhoff, Salditt NJP 2011

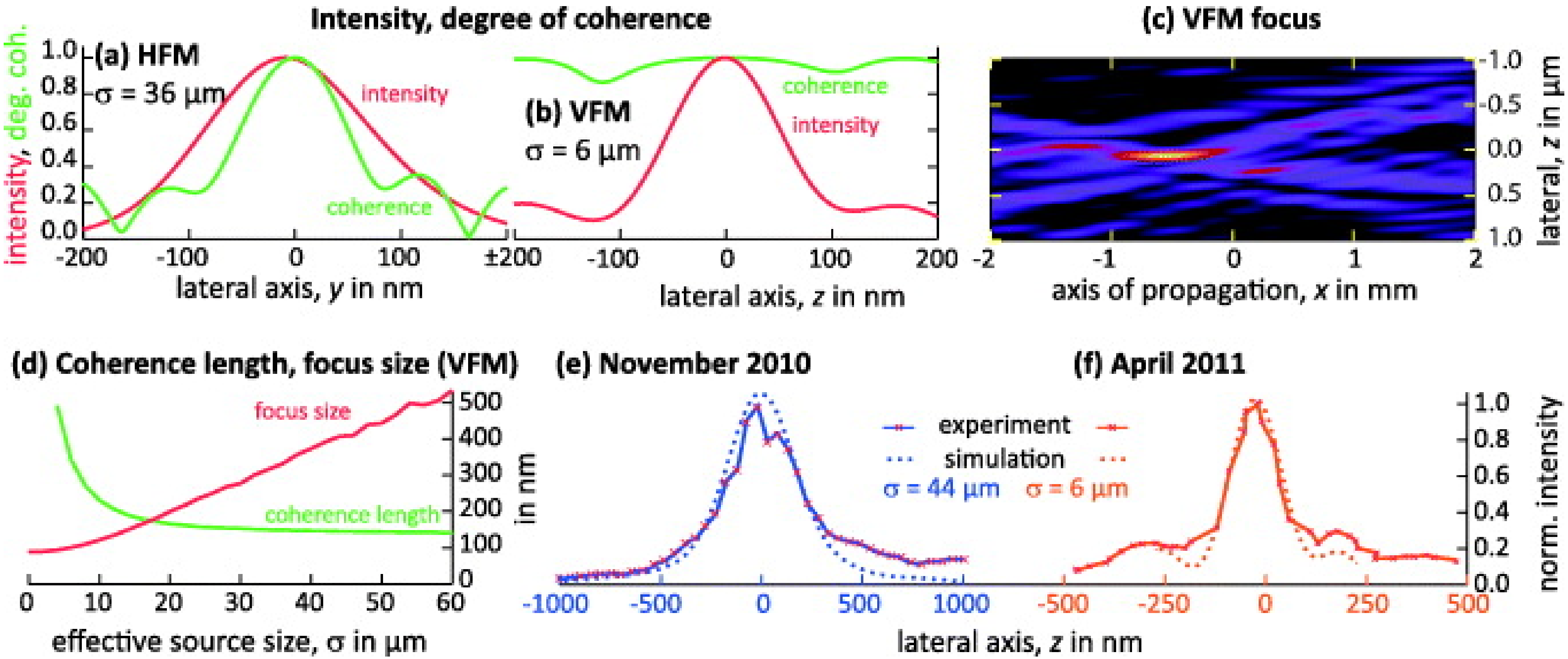

Osterhoff, Salditt NJP 2011

measured coherence function in good agreement with simulation

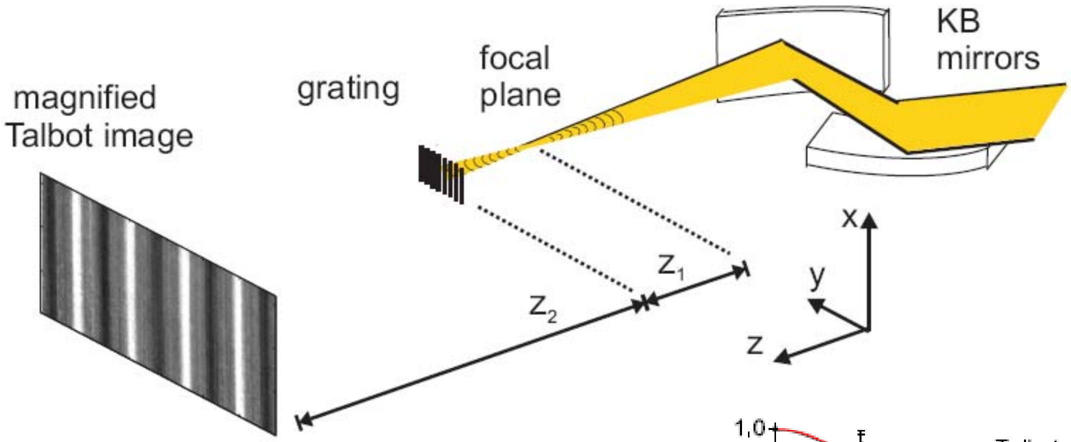

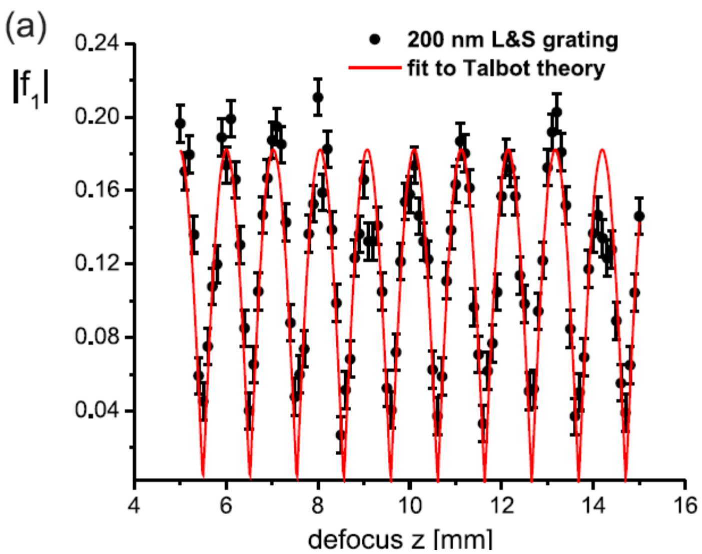

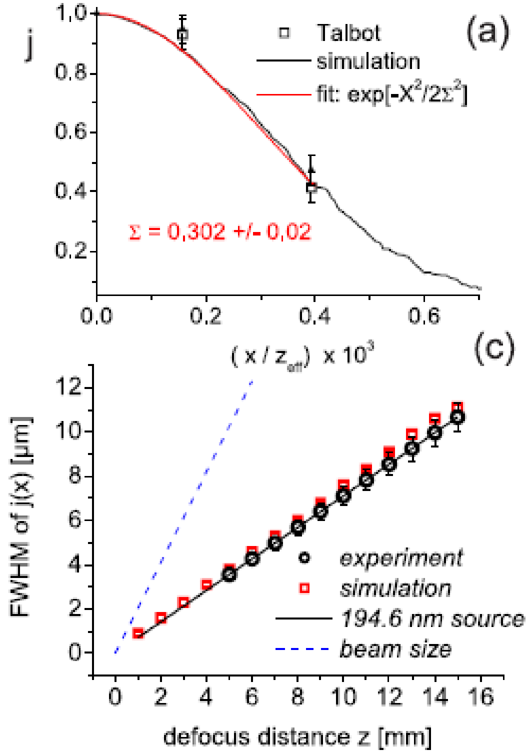

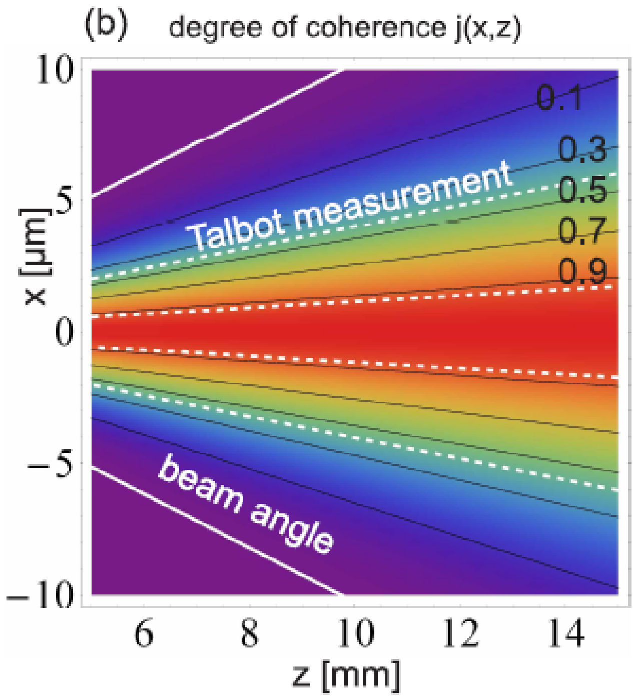

T. Salditt et al. Opt. Express 2011

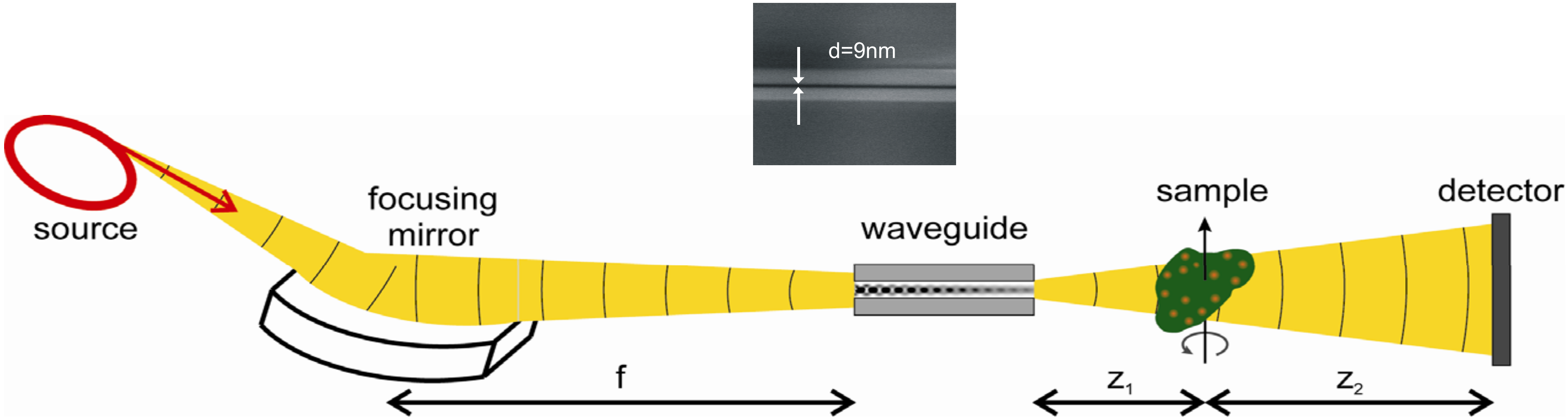

Coupling of mirrors beam into waveguide …

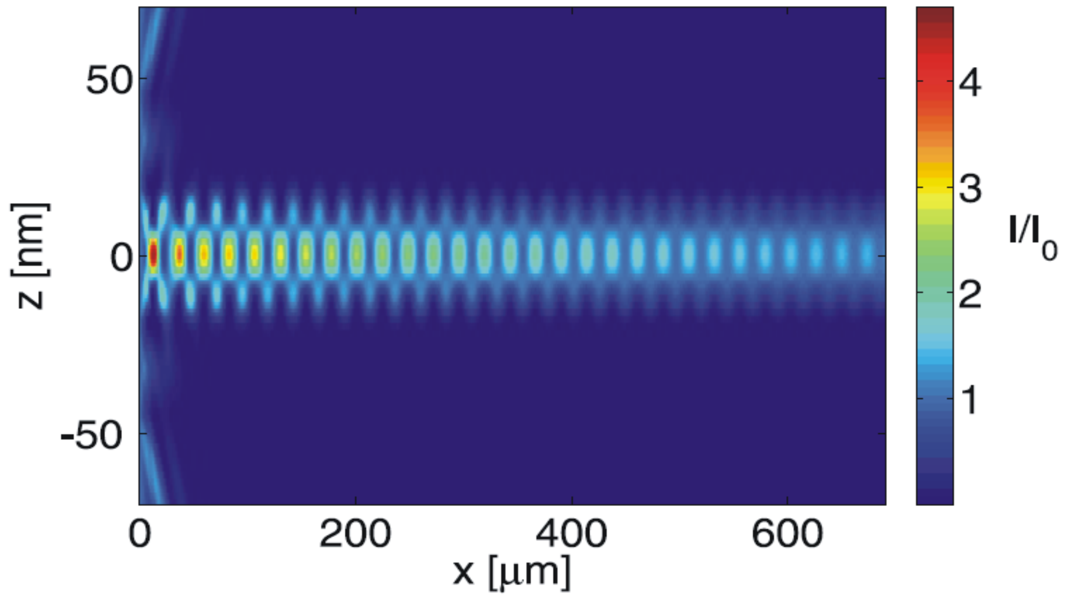

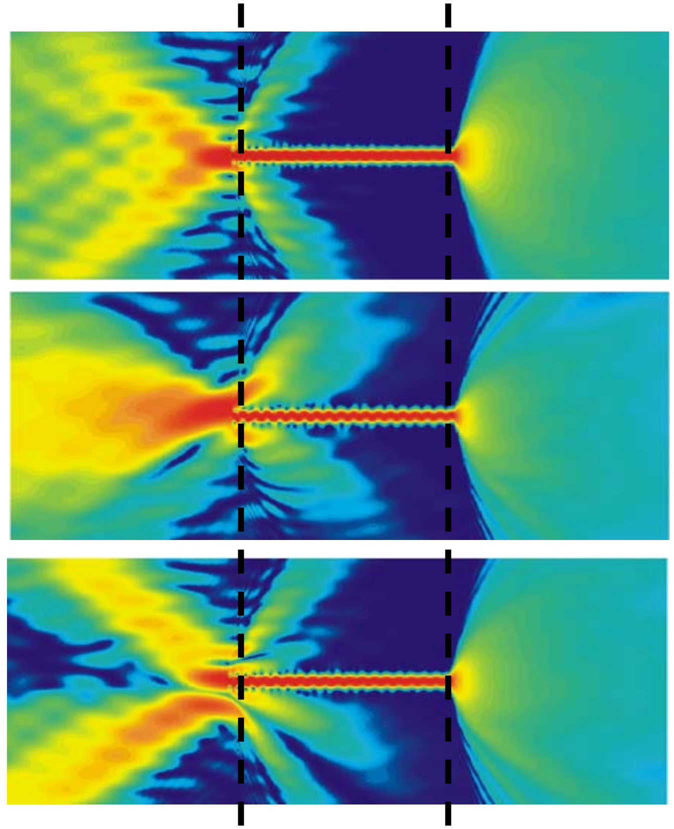

Osterhoff, Salditt NJP 2011

X-ray waveguide optics

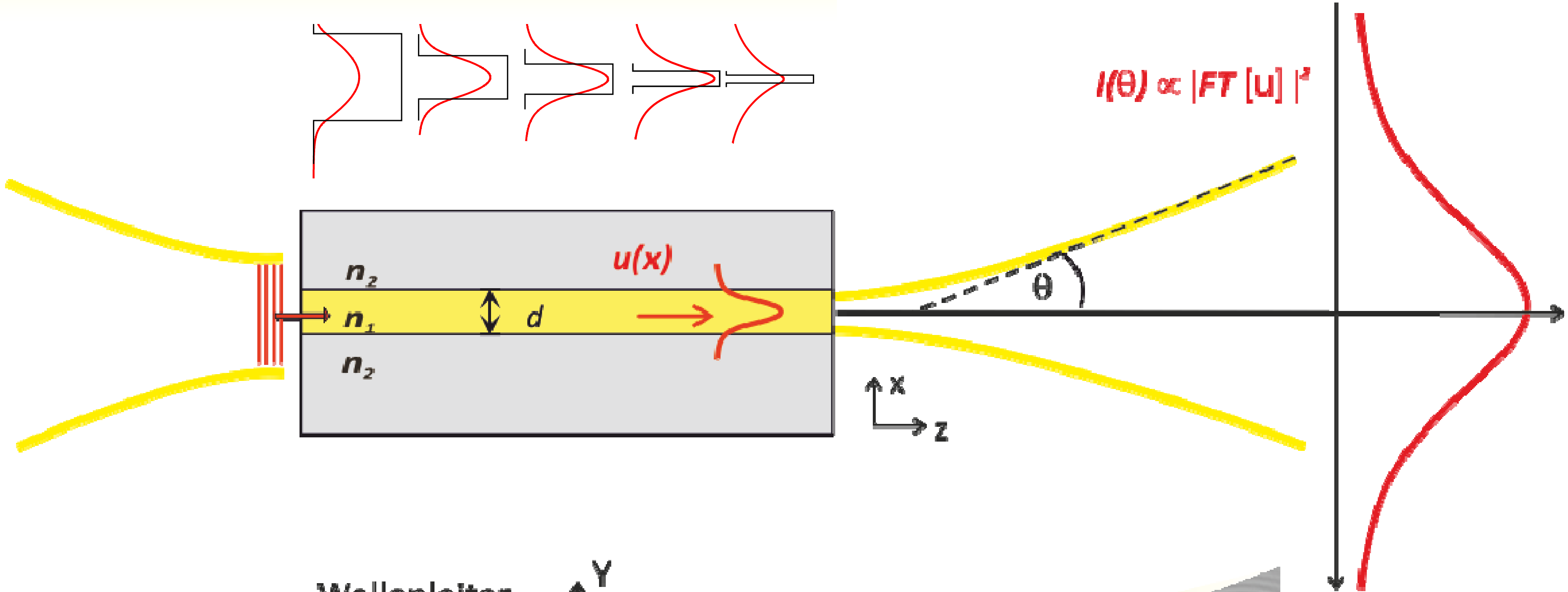

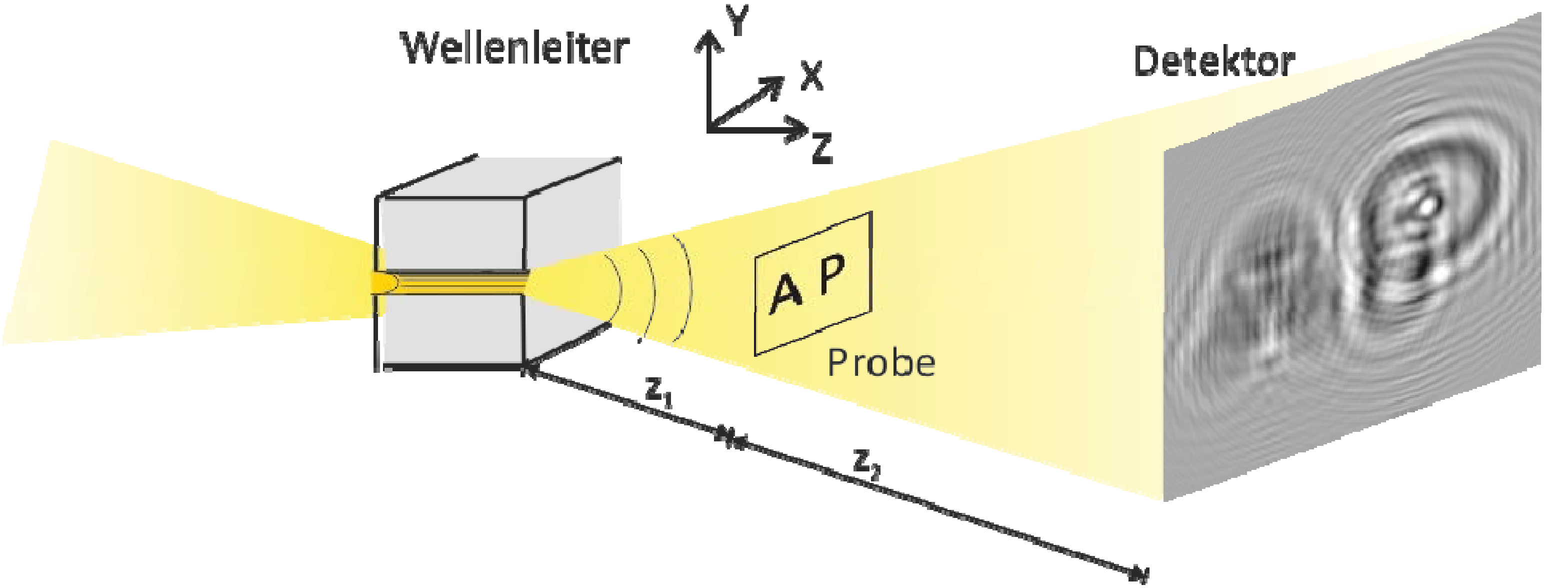

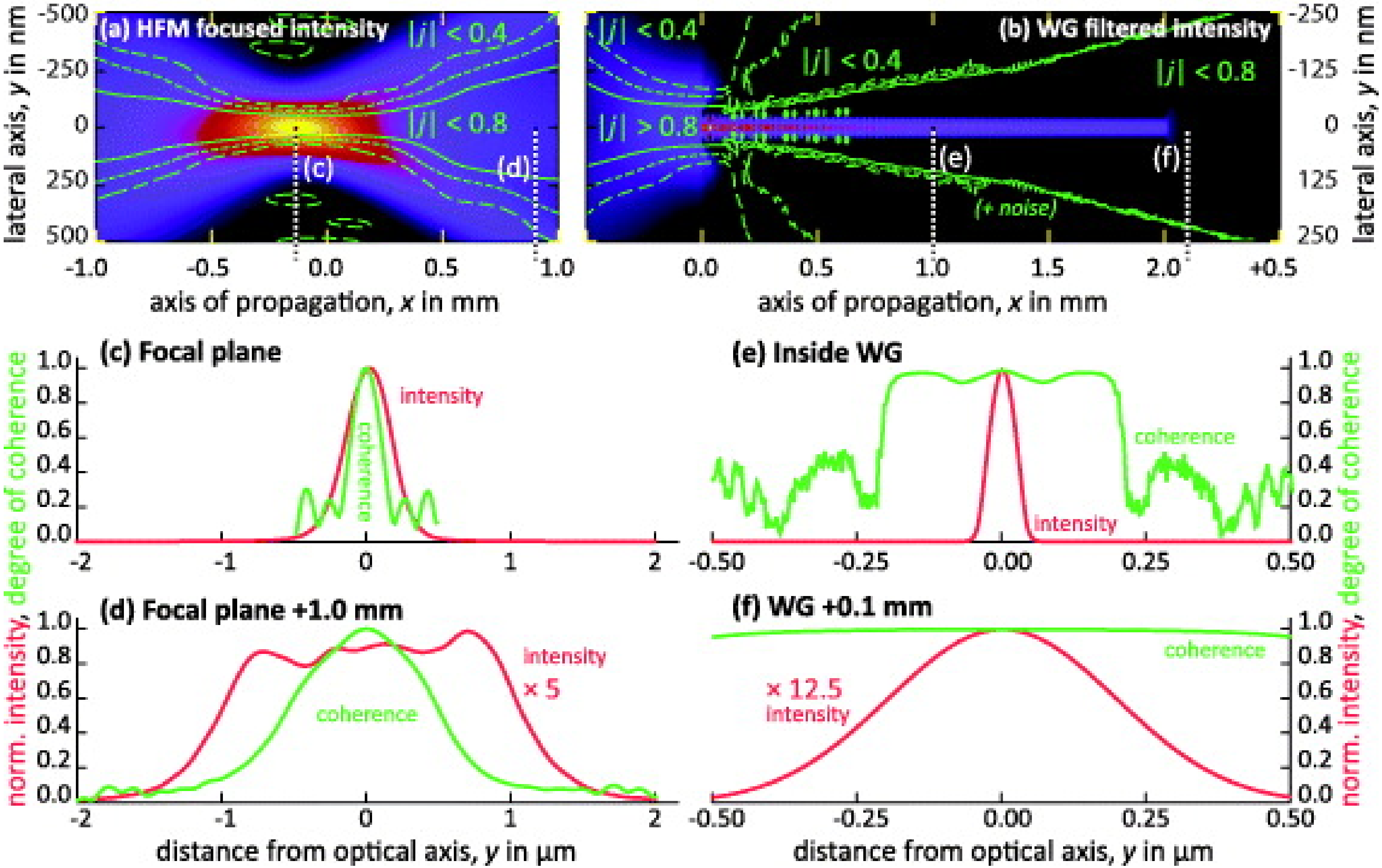

Osterhoff, Salditt NJP 2011

New generations of x-ray waveguides: (a) crossed high transmission planar waveguides (b) lithographic channels in Si sealed by wafer bonding

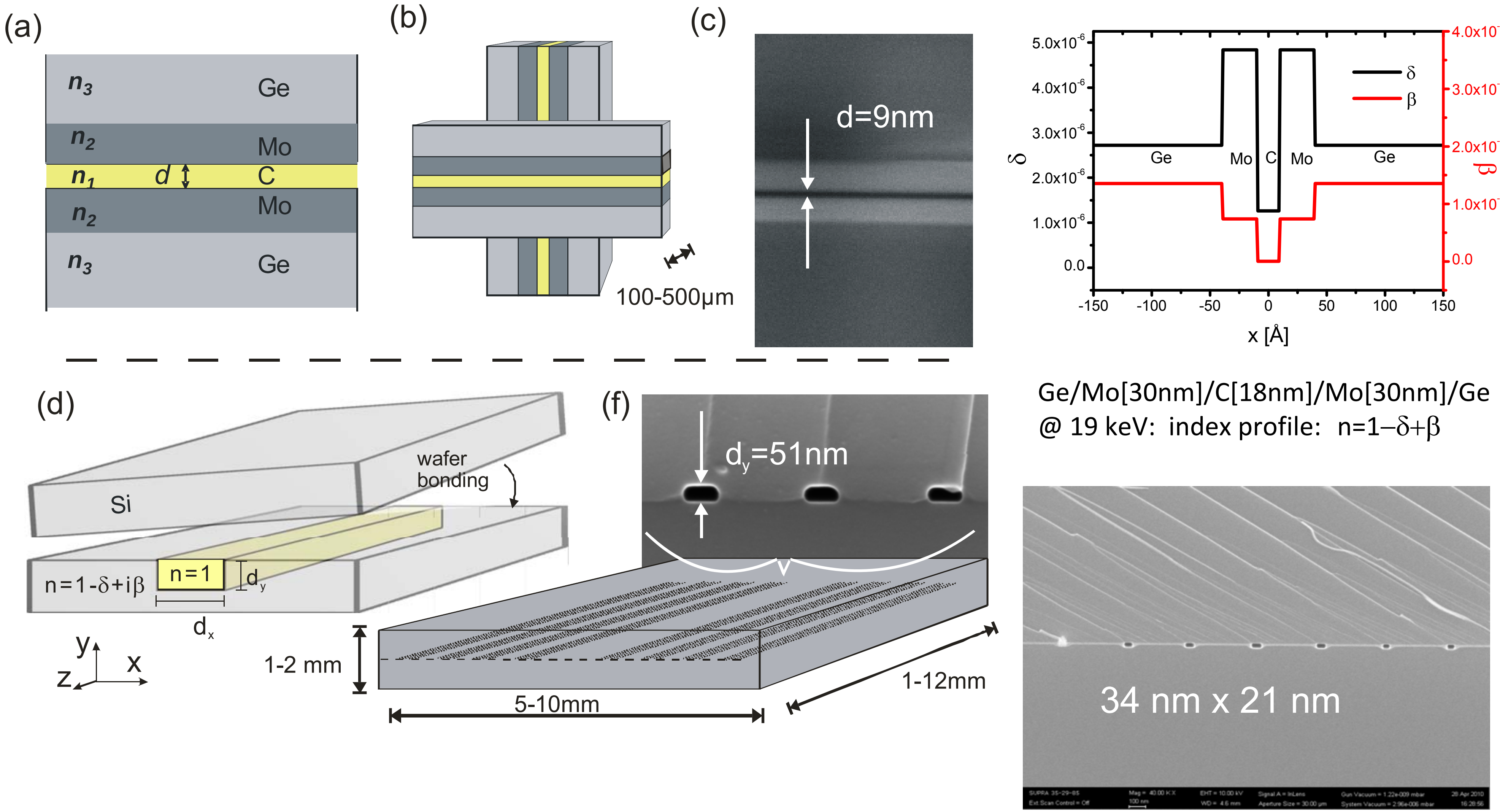

T. Salditt, S. Krüger, C. Baehtz, Phys. Rev. Lett. 2008; S. Krüger et al., Opt. Express 2010; H. Neubauer, M. Kanbach et al., unpublished

Waveguide based propagation imaging

Waveguide system

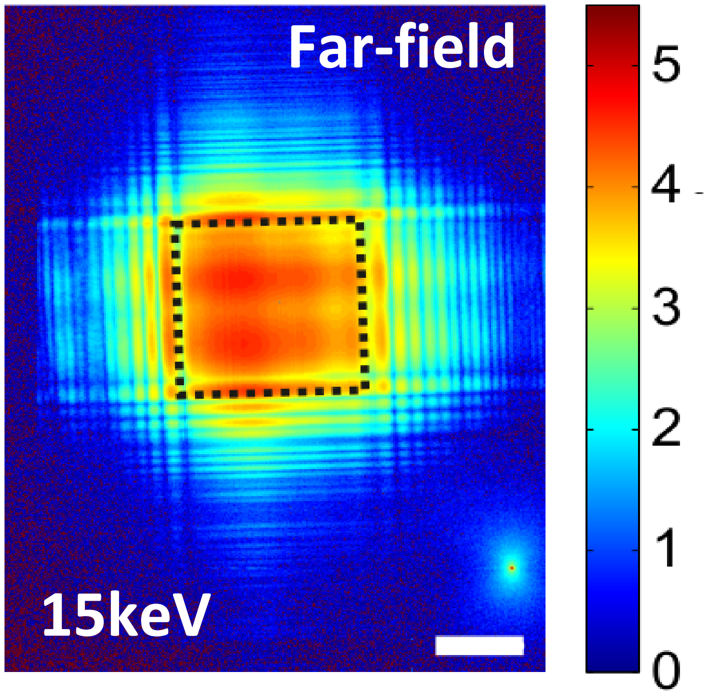

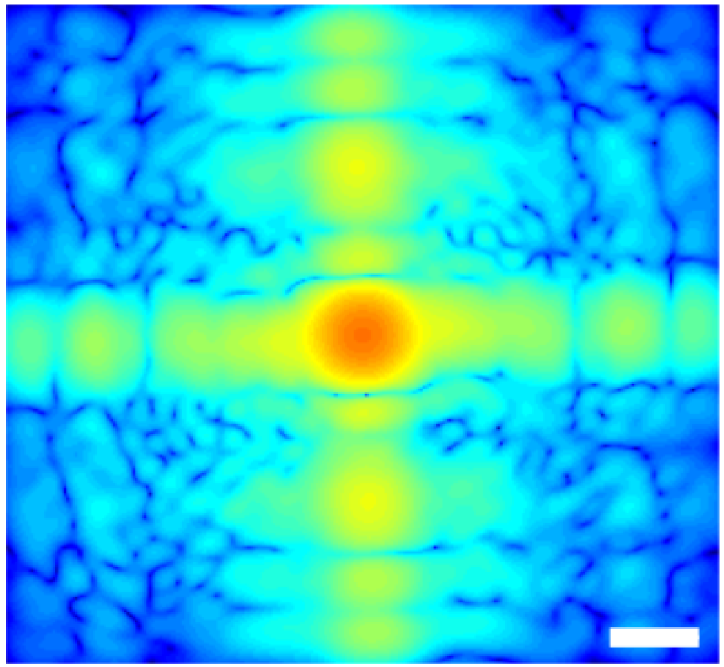

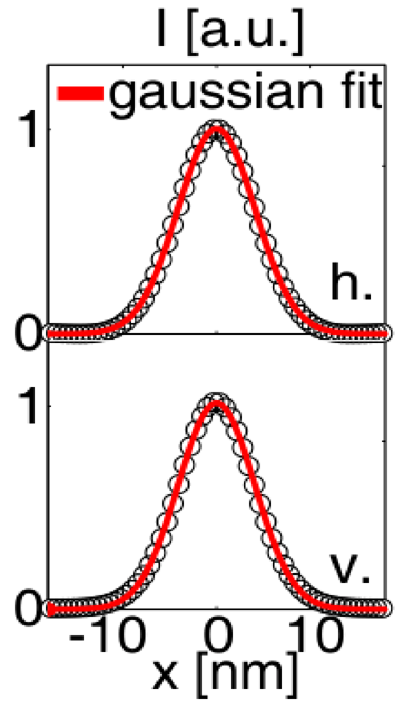

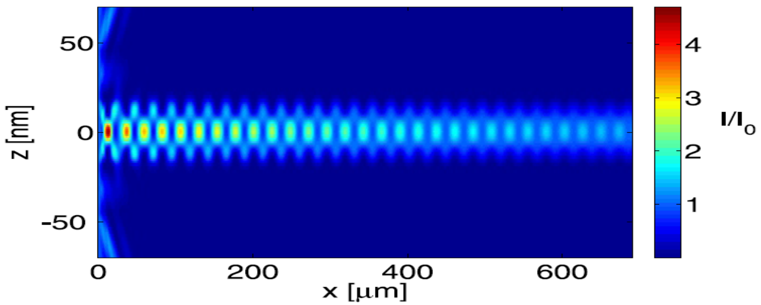

Effective focal plane

10 nm x 9.8 nm (FWHM)

1e7 cps

Calculation of near-field intensity distribution from farfield diffraction pattern: *sub 15 nm beam size in two dimensions*

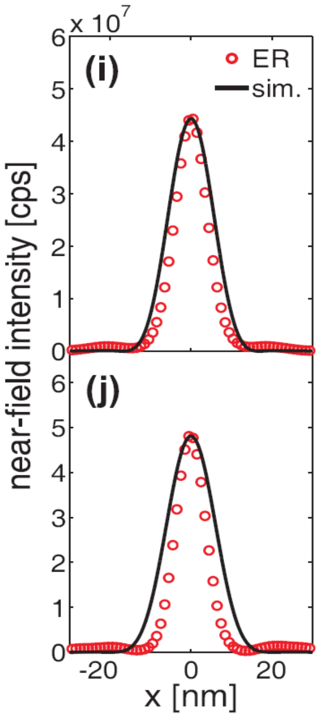

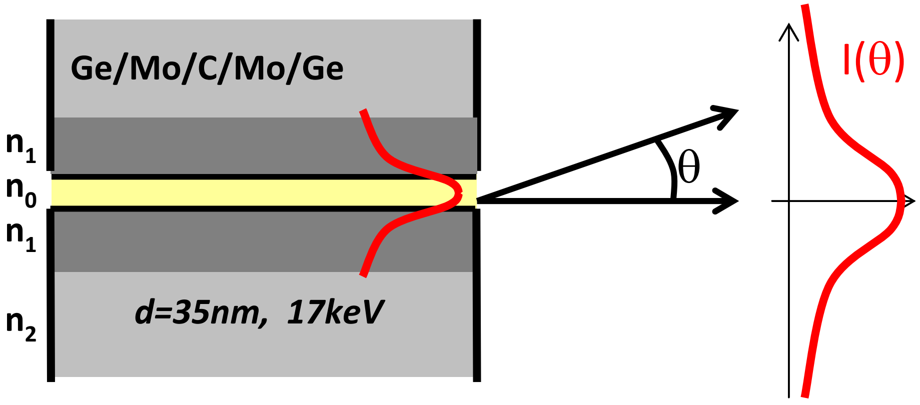

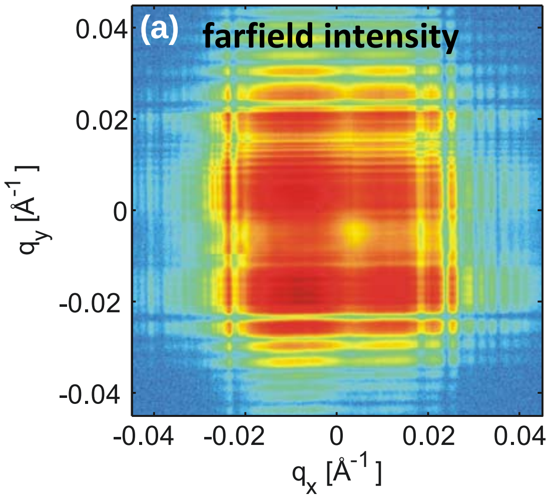

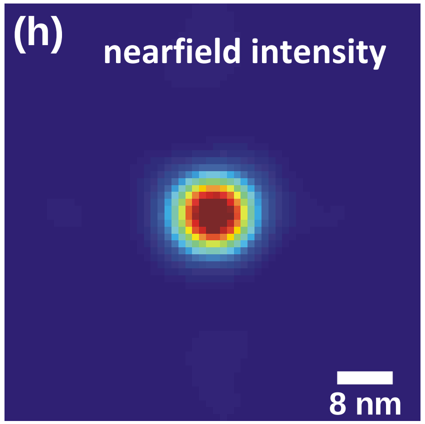

error reduction (ER) algorithm

$g_i(x)$

$g_i(x) \xrightarrow{FT} G_i(k)$

$G_i(k) = |G| e^{i\phi} \rightarrow G'_i(k) = |F(k)| e^{i\phi}$

$G'_i(k) = |F(k)| e^{i\phi} \xrightarrow{FT^{-1}} g'_i(k)$

$g_{i+1}(x) = g'_i(k)$ inside support

$= 0$ outside support

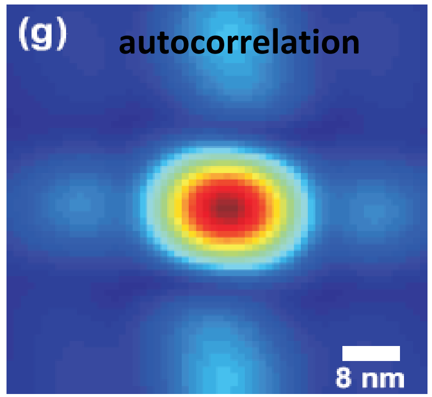

<u>beam size (FWHM vert x horz)</u>

reconstruction: 9.2nm x 9.6 nm

simulation: 12.5nm x 13.6 nm

autocorrelation: 14.2nm x 17.9 nm

S. Krüger *et al.*, Optics Express, 2010

world record in one-dimension: 7nm focus
by EEM polished mirror @1km long beamline 29 Spring8
(Yamauchi group, Osaka Univ.)

H. Mimura *et al.*, Nature Physics, 2010
Breaking the 10 nm barrier in hard x-ray focusing

X-ray imaging of cells: *Dictyostelium Discoideum*

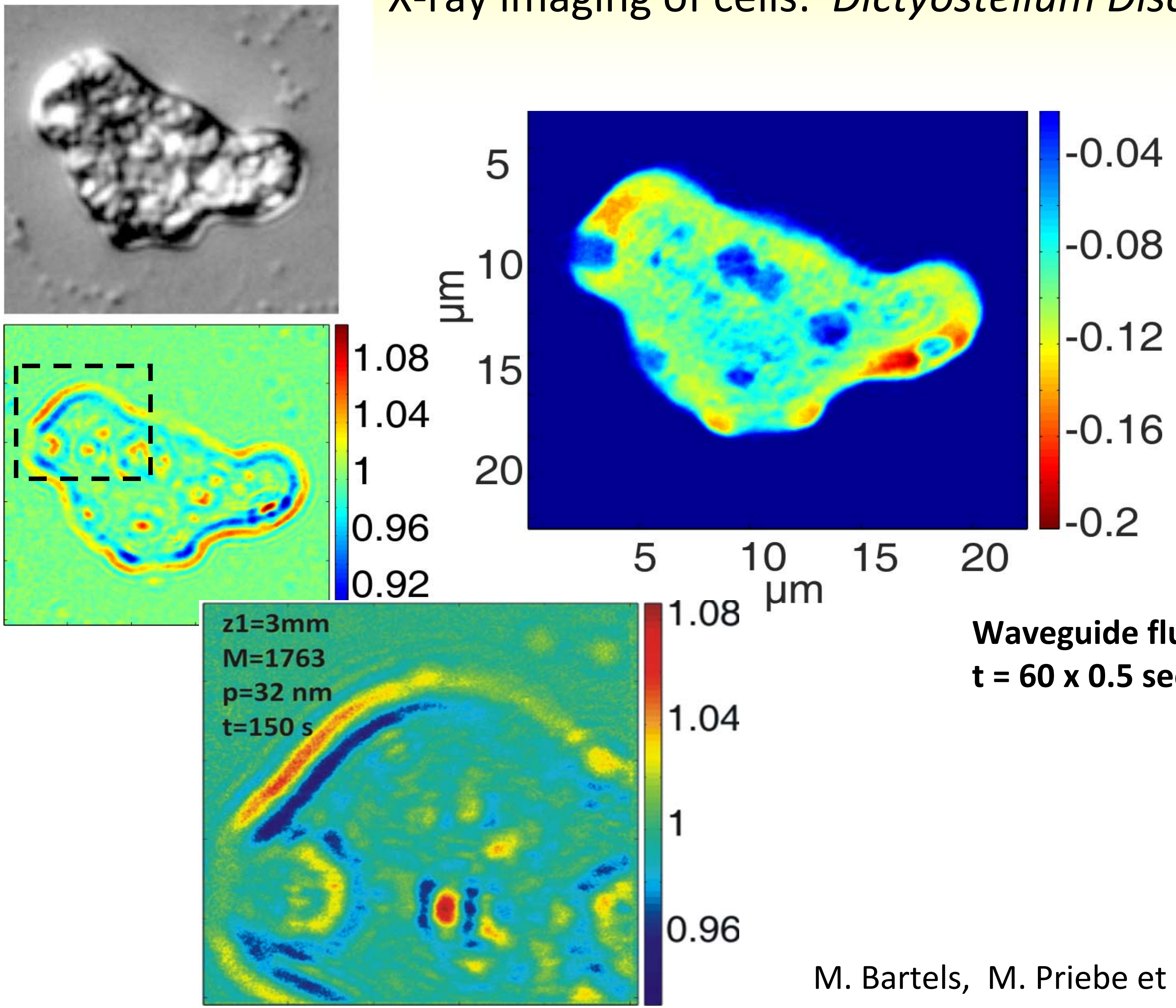

Waveguide flux = 1e8 ph/s
t = 60 x 0.5 sec = 30 sec

M. Bartels, M. Priebe et al., unpublished

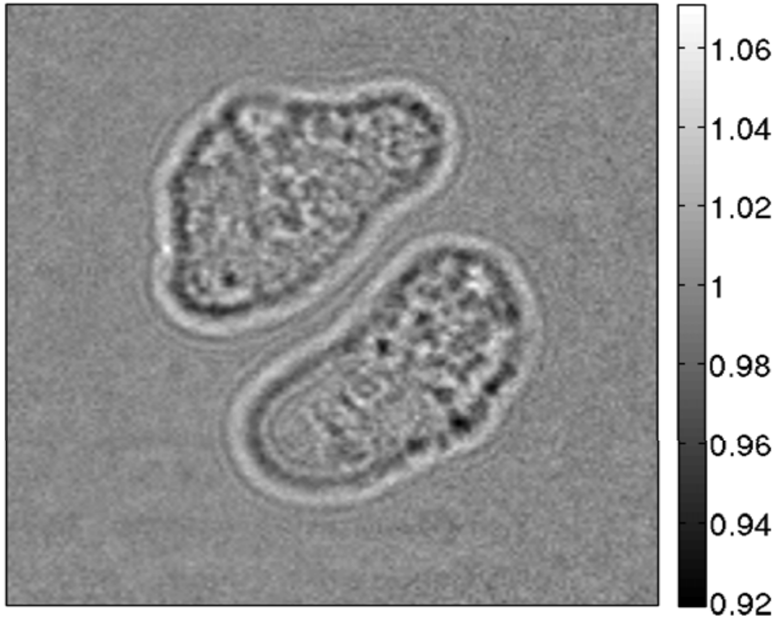

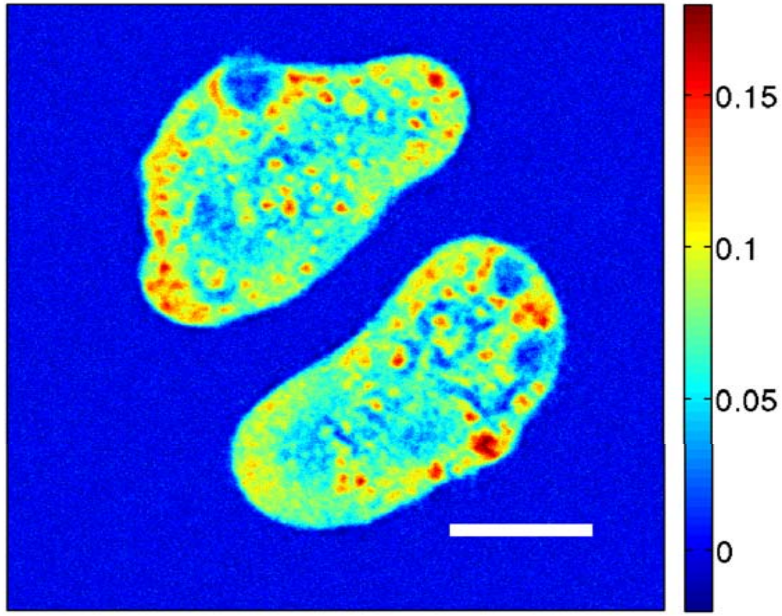

ID 22NI, 17.5 keV
35 x 35 nm crossed WG
8.3 mm defocus

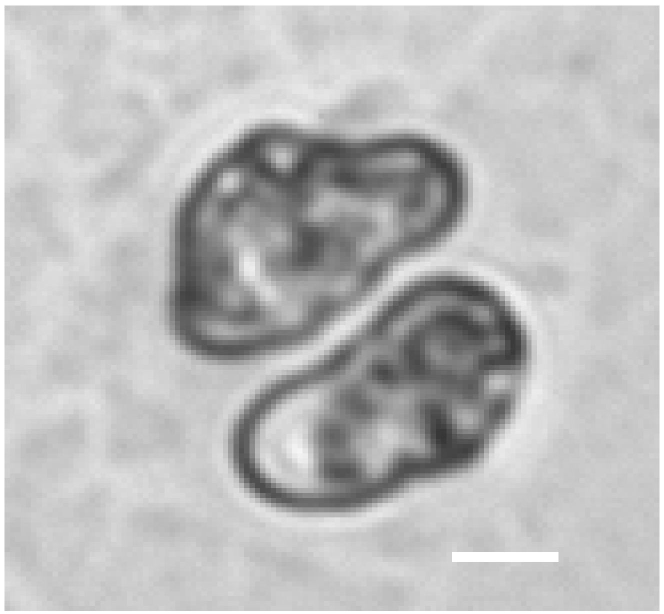

Zellen
(*Dictyostelium Discoideum, cryo. fixiert & gefrier getrocknet*)

- Phaseninformation durch Referenzwelle
- quantitativer Dichtekontrast
- iterative Rekonstruktion
- Lösung des Zwillingsbildes (hologr. Artifakt)

K. Giewekemeyer ,S. Krüger, S. Kalbfleisch,
M. Bartels, C. Beta, T. Salditt , Physical Review A, 2011

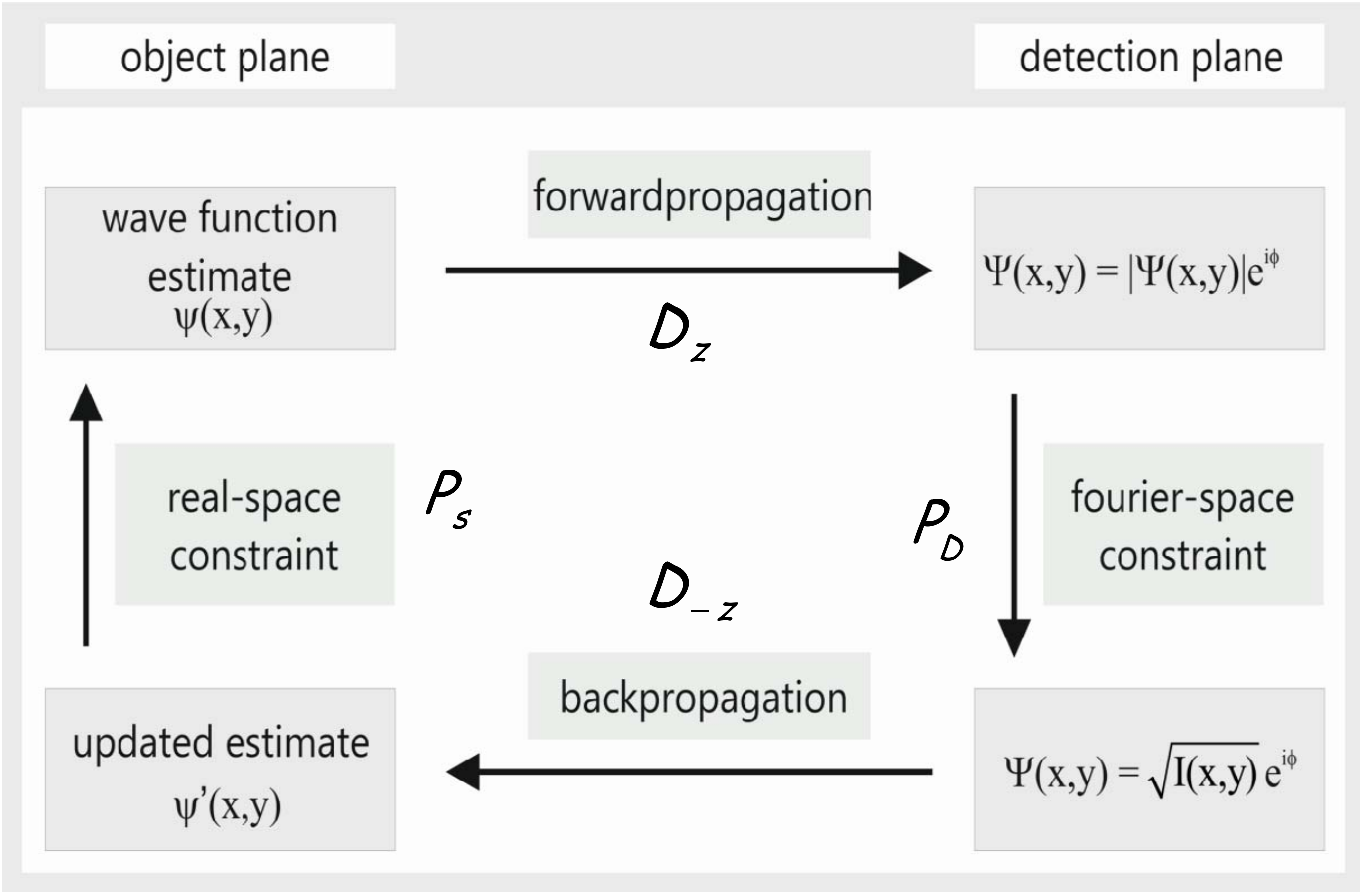

Propagator $D_z = FFT^{-1} \exp[\, iz\sqrt{k^2 - k_x^2 - k_y^2}\,]\; FFT$

P_s : projector in sample plane

$$\left|\chi_{n+1}(x,y)\right| = \left|\chi_n(x,y)\right| - \beta\left(\left|\chi'_n(x,y) - 1\right|\right)$$

$$\arg(\chi_{n+1}(x,y)) = \begin{cases} \arg(\chi_n) - \gamma \arg(\chi'_n) & \forall (x,y) \notin S \\ \min(\arg(\chi'_n, 0)) & \forall (x,y) \in S \end{cases}$$

S support (from holographic reconstruction)

P_D :'projector' in detector plane

$$\left|\tilde{\chi}'_n(x,y)\right|^2 = \left(1 - \frac{D}{d}\right)\bar{I}(x,y) + \frac{D}{d}\left|\tilde{\chi}_n(x,y)\right|^2$$

$$d^2 = \frac{1}{N}\sum_{x,y}\left(\left|\tilde{\chi}_n(x,y)\right|^2 - \bar{I}(x,y)^2\right)^2$$

$D = \sqrt{2 / \langle I_0 \rangle}$ noise

X-ray imaging of bacterial **cells**
Deinococcus Radiodurans

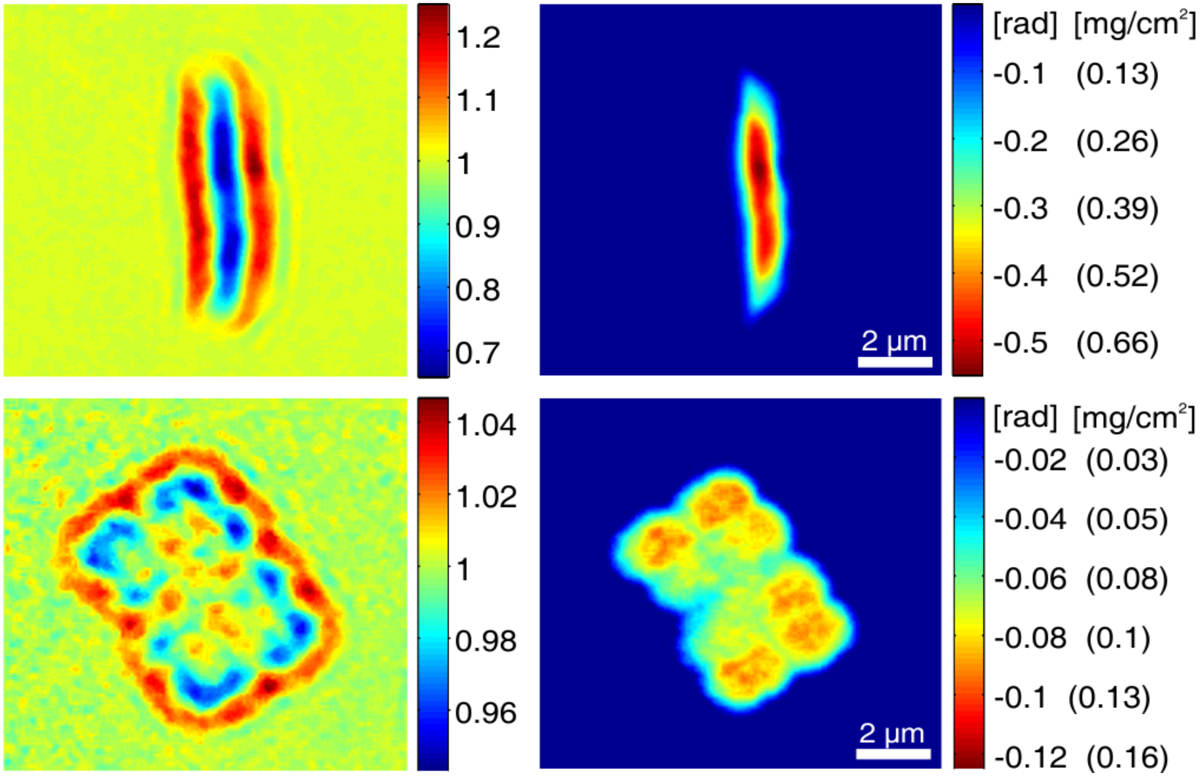

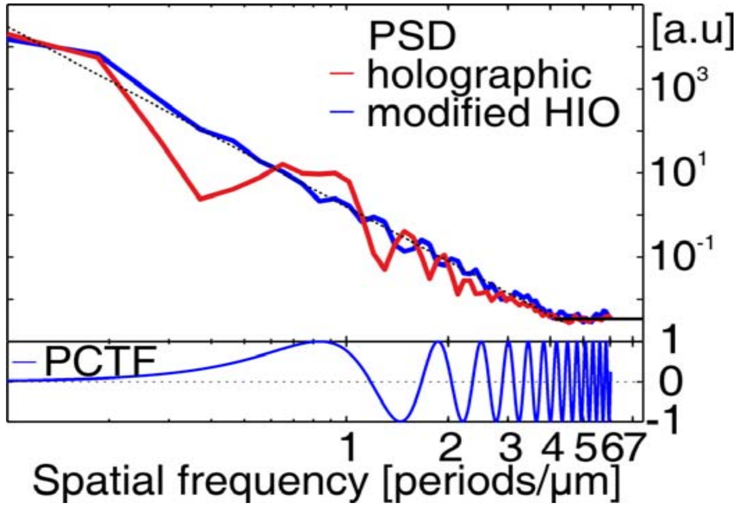

E=13.8 keV
z1=8 mm
z2=5.3 m
M=660
P=55 µm
p=83 nm
t=10 min
F=2.6e5 ph/µm²
D=110 Gy
r=125 nm

M.Bartels, M. Priebe et al., submitted.

DNA packing in nucleoids: Tomography of *Deinococcus Radiodurans*

- **Among most radiationresistant organisms on earth, can survive 15 kGy of ionizing radiation**
- **Very effective DNA repair mechanism, DNA packing debated**

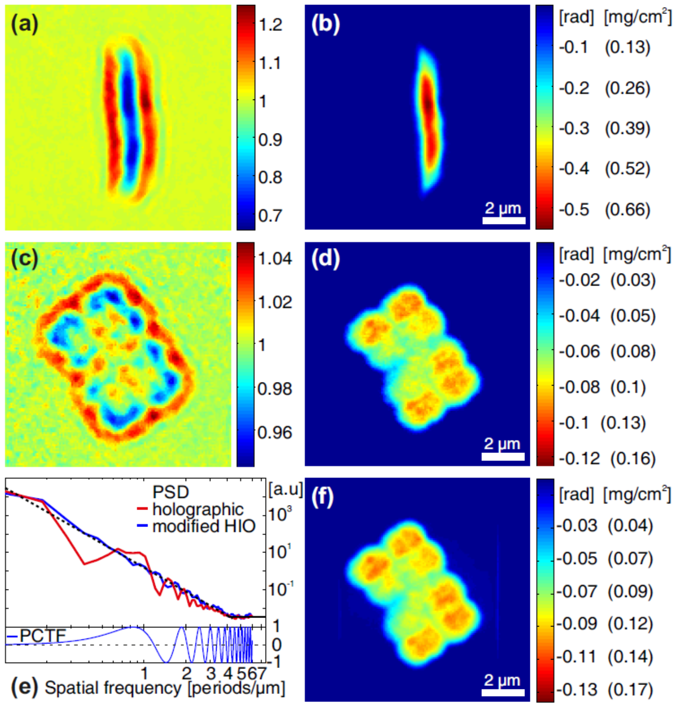

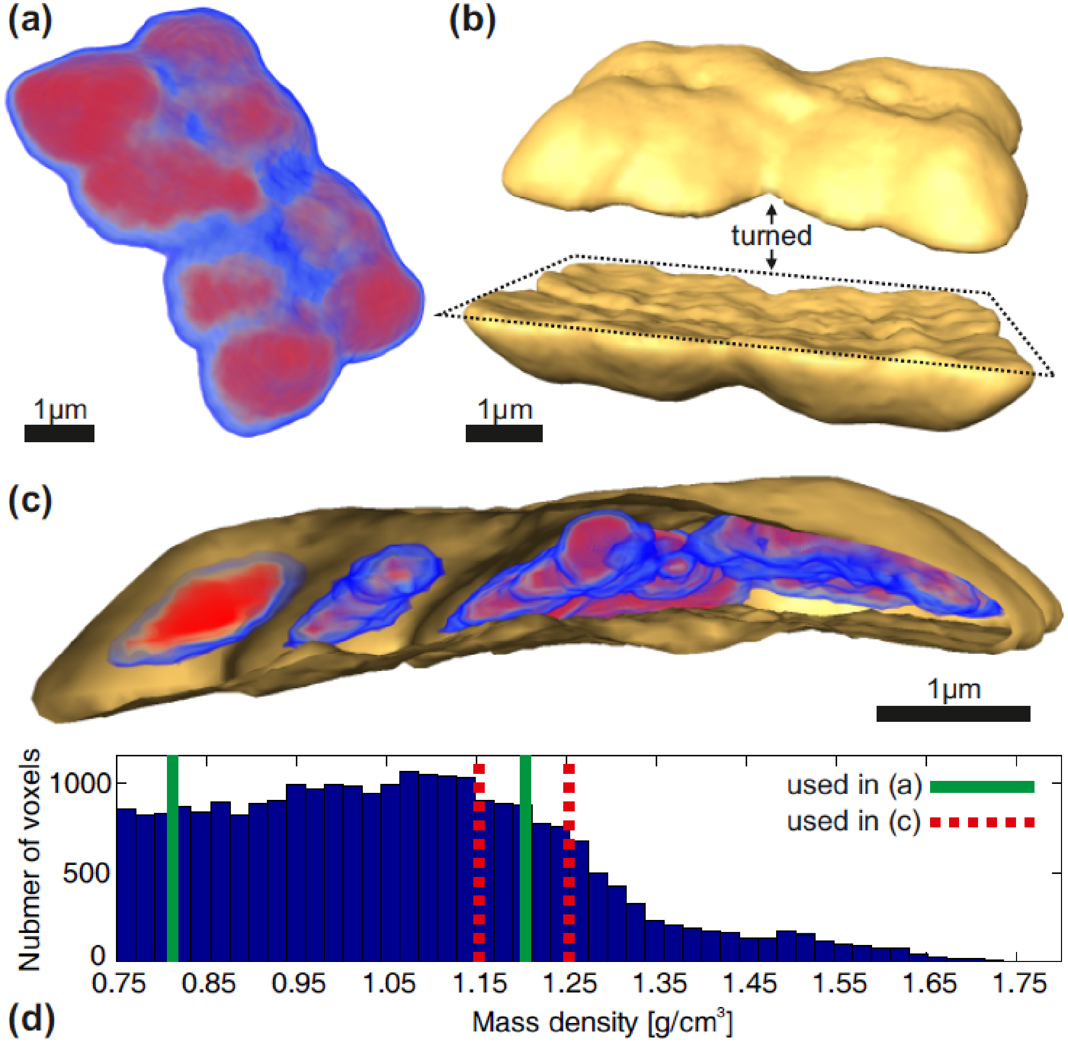

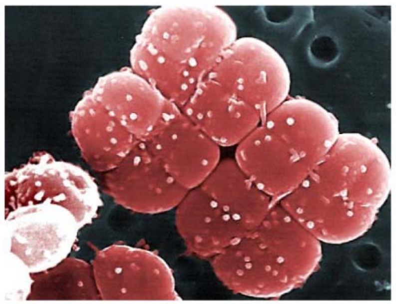

2x3 µm size, tetrad morphology
4 identical copies of the genome

Matthias Bartels et al. (unpublished manuscript)

PRL 102, 018101 (2009) PHYSICAL REVIEW LETTERS week ending 9 JANUARY 2009

Three-Dimensional Visualization of a Human Chromosome Using Coherent X-Ray Diffraction

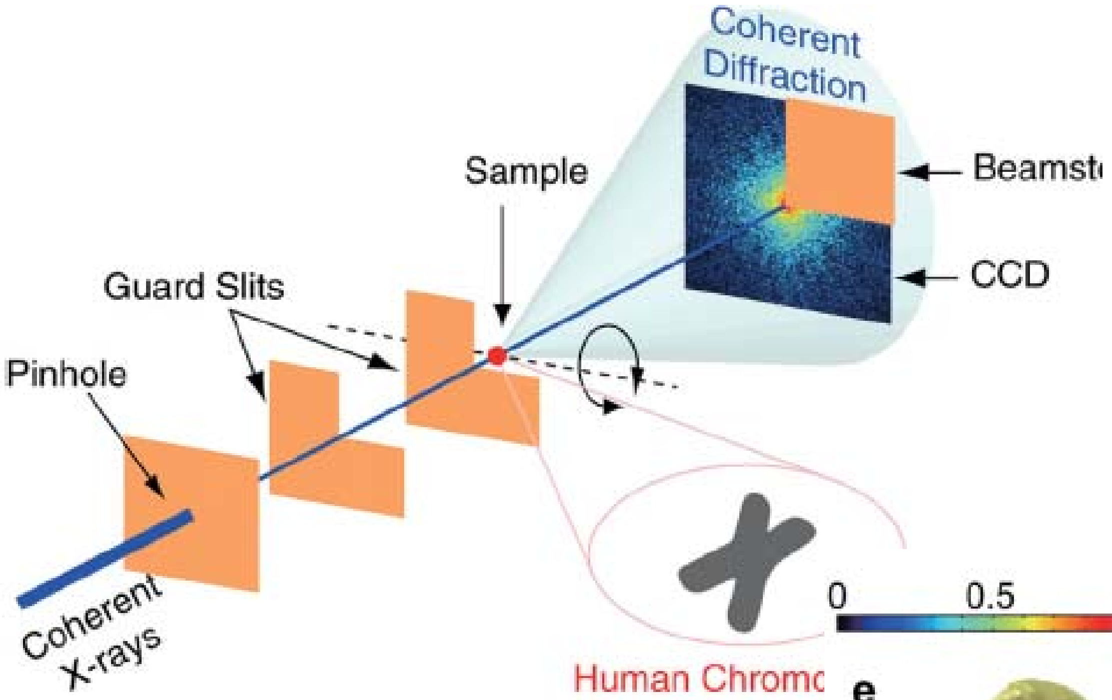

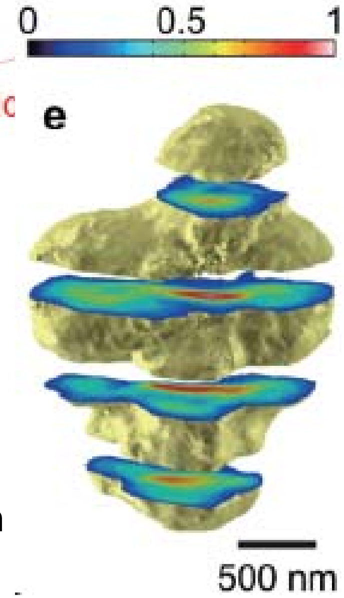

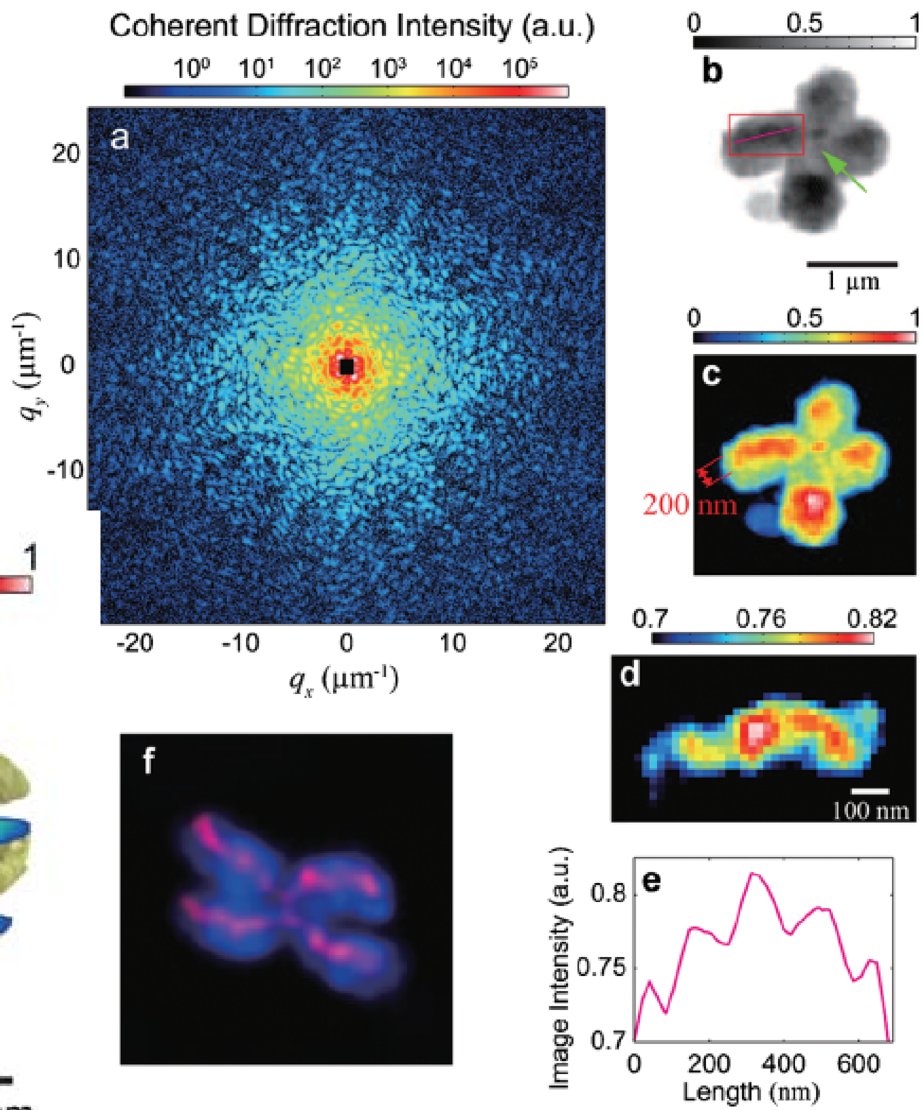

freeze dried Chromosomes from HELA cells
Flux: 10^{10} cps in 33µm (5 keV)
accumulation time: 2700s per projection
56 projections
resolution of 2D projection image: ~ 30nm
resolution of the 3D reconstruction: ~ 120 nm
radiation dose (tomography) : 2 10^{10} Gy
results: chromatin, heterochromatin in centromere

FIG. 2 (color). Coherent diffraction pattern of an unstained human chromosome and its reconstructed projection image. The

X-ray propagation imaging
Dose efficiency

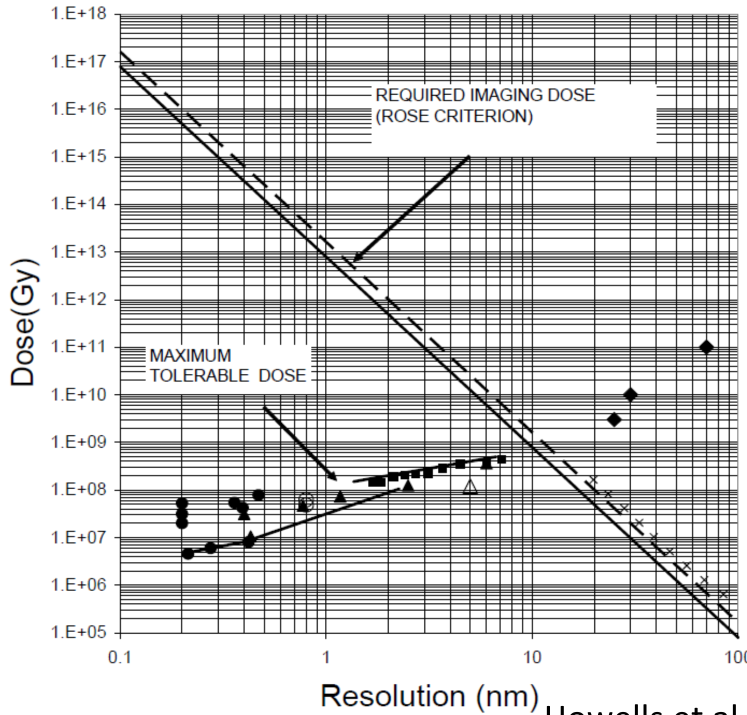

Howells et al., 2009

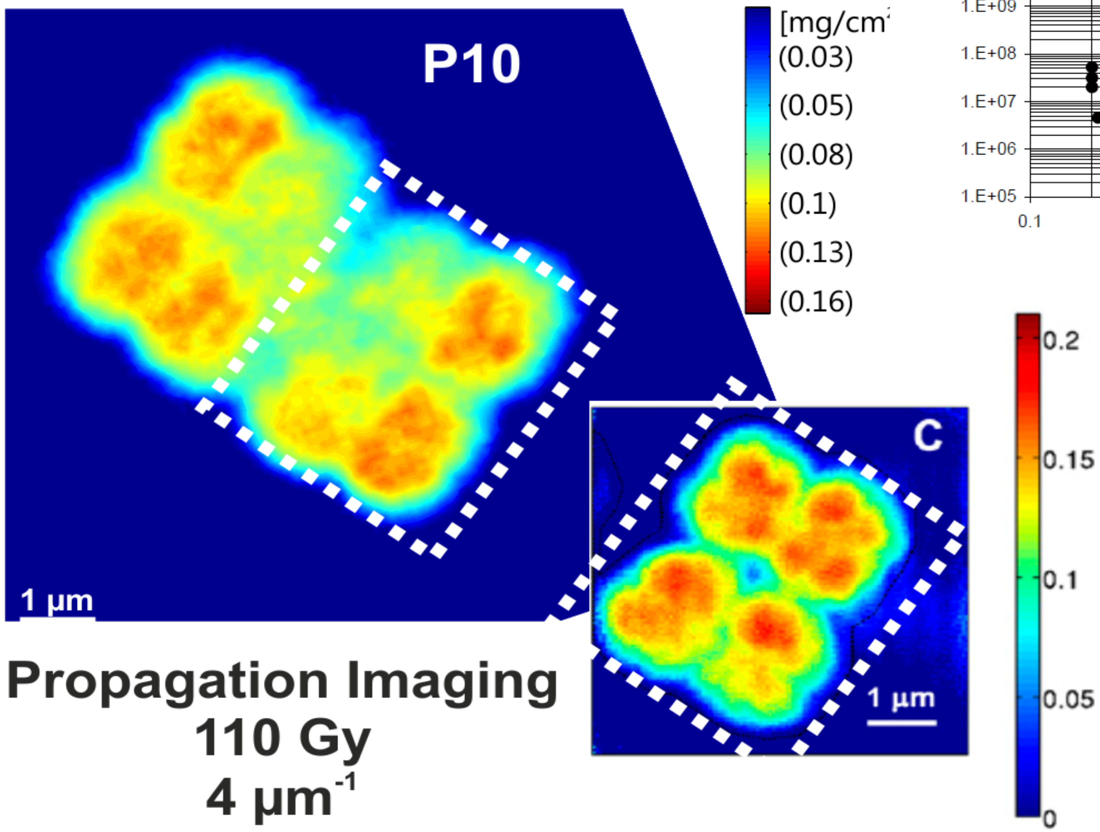

Propagation Imaging
110 Gy
4 µm^{-1}

Ptychography*
1.3e5 Gy
5.9 µm^{-1}

K. Giewekemeyer et al., PNAS 2010

The advent of x-ray free electron lasers *9 orders in peak brilliance !*

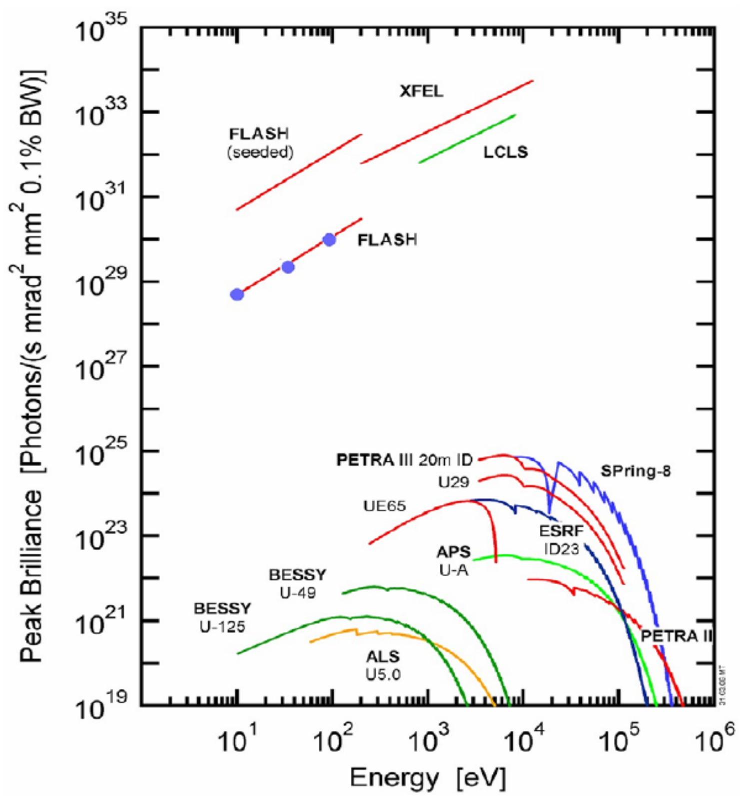

Figure 1. Peak brilliance of storage ring and FEL sources.

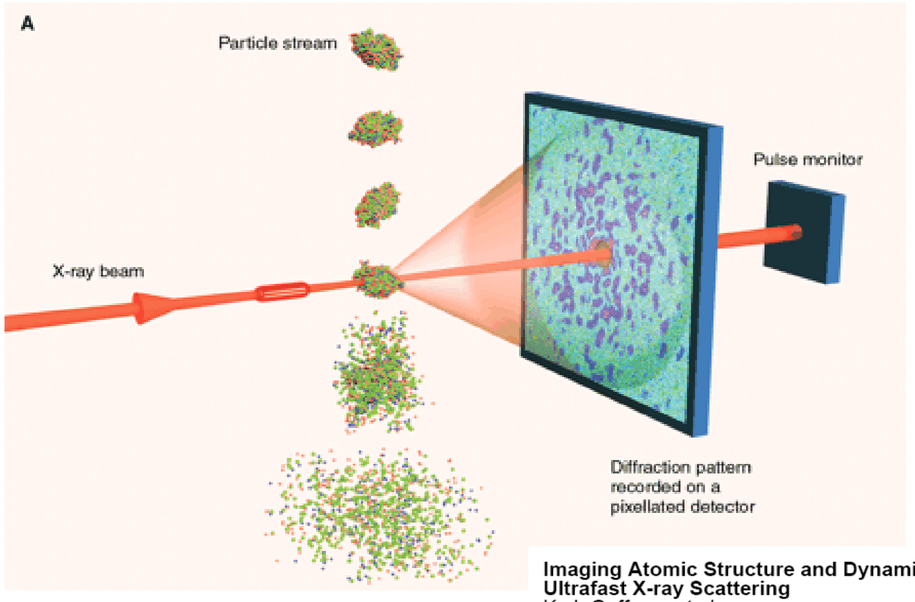

Imaging Atomic Structure and Dynamics with Ultrafast X-ray Scattering
K. J. Gaffney, *et al.*
Science **316**, 1444 (2007);

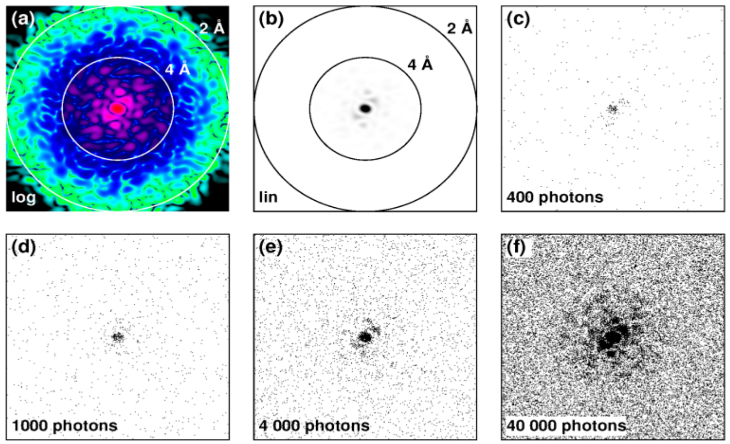

Simulated diffraction images of a single molecule in different representations (a)+(b) and at different intensities (c)-(f).

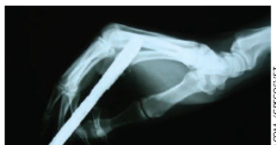

editorial

X-ray vision

The century-old field of X-ray physics is being rejuvenated by new forms of ultrabright sources based on laser technology, promising a revolution in imaging capabilities.

This month *Nature Photonics* presents a special Focus Issue dedicated to the latest advances in X-ray optics, a field that has a long and rich history.

"I have seen my death," exclaimed Anna Röntgen in mid-November, 1895. She had just seen the first ever human X-ray image — a picture of her own hand revealing the bones beneath the flesh.

setting, using either high-harmonic generation, laser wakefield or various types of plasma sources. This is in stark contrast with the immobile nature of synchrotrons, in which most high-resolution work has been done so far. X-ray imaging schemes generally utilize soft X-rays or high-spatial-resolution hard X-rays, with or without lenses, in a modality that is

C10 (Salditt /Köster)
Single pulse cellular imaging (high throughput)

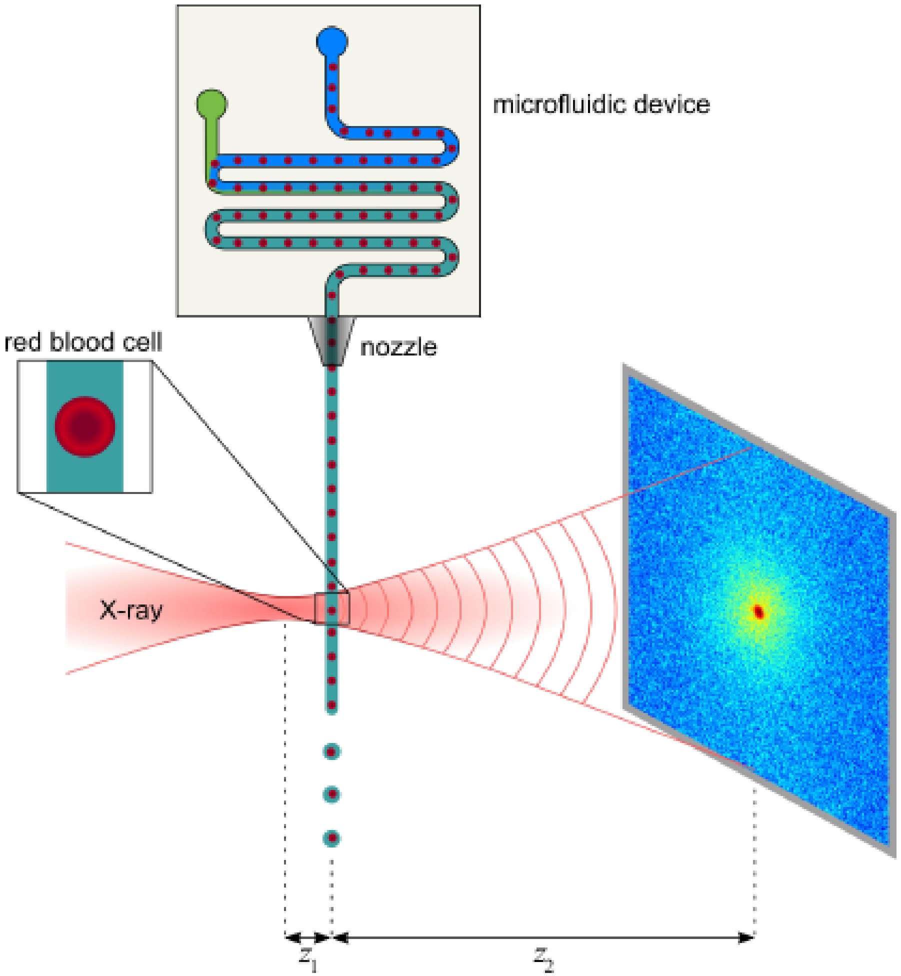

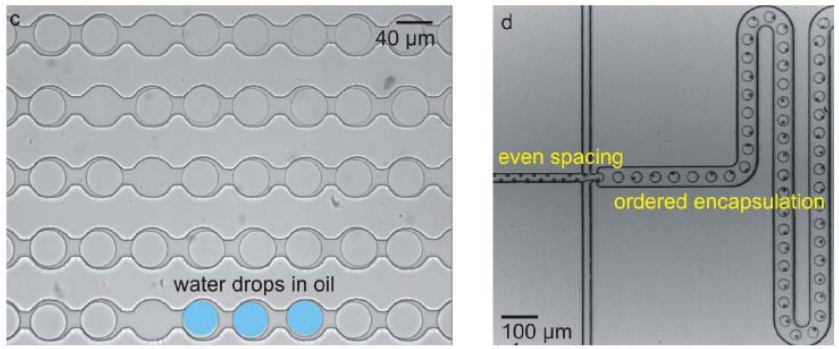

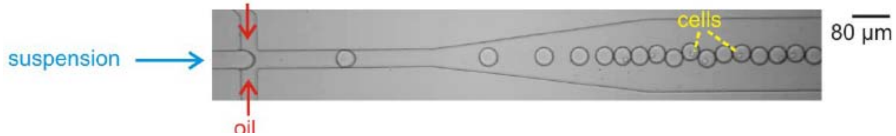

$N_0 = 10^{12} \quad photons\,/\,pulse$

assume $N_c = 10^5$ per resolution element r

$\rightarrow$ 3000x3000 pixel in field of view V

$\lambda = 0.1\text{nm}, \text{V} = 10\mu\text{m}, \ \text{z}_1 = 10mm, r = 3nm$

focus $\Delta = 100nm$

fluence at defocus $N_0 \lambda^2 \Delta^2 / z_1^2$

3D information from anlylography ?

$\rightarrow @10^8 \ W/cm^2$:

$100mV$ transmembrane Voltage

FEL – Liquid Jet

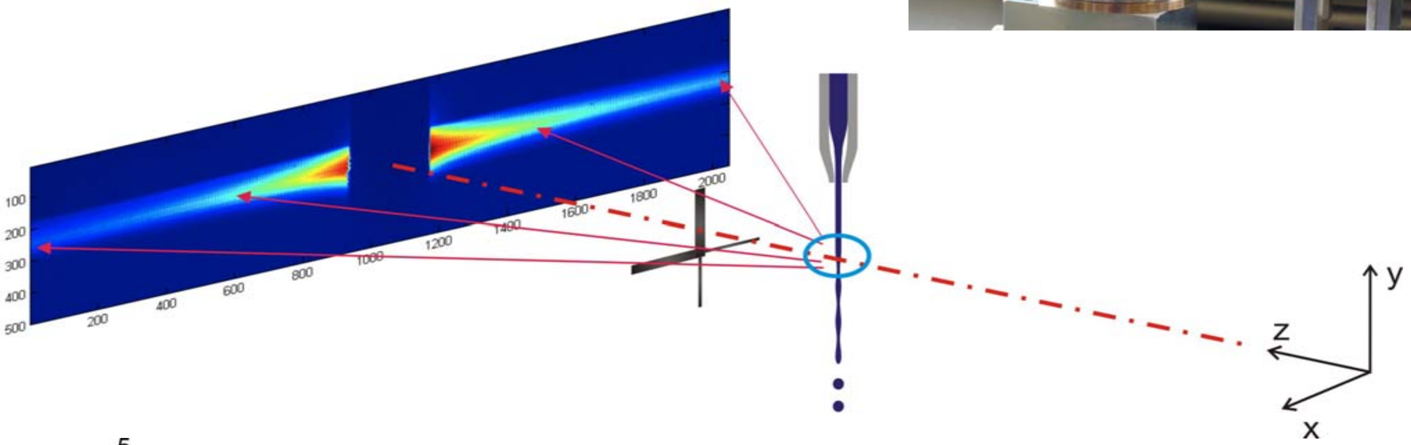

FEL

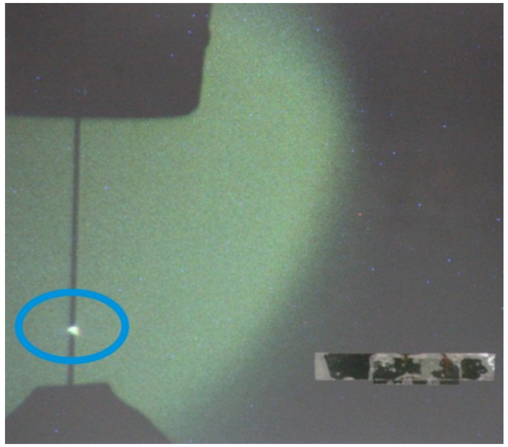

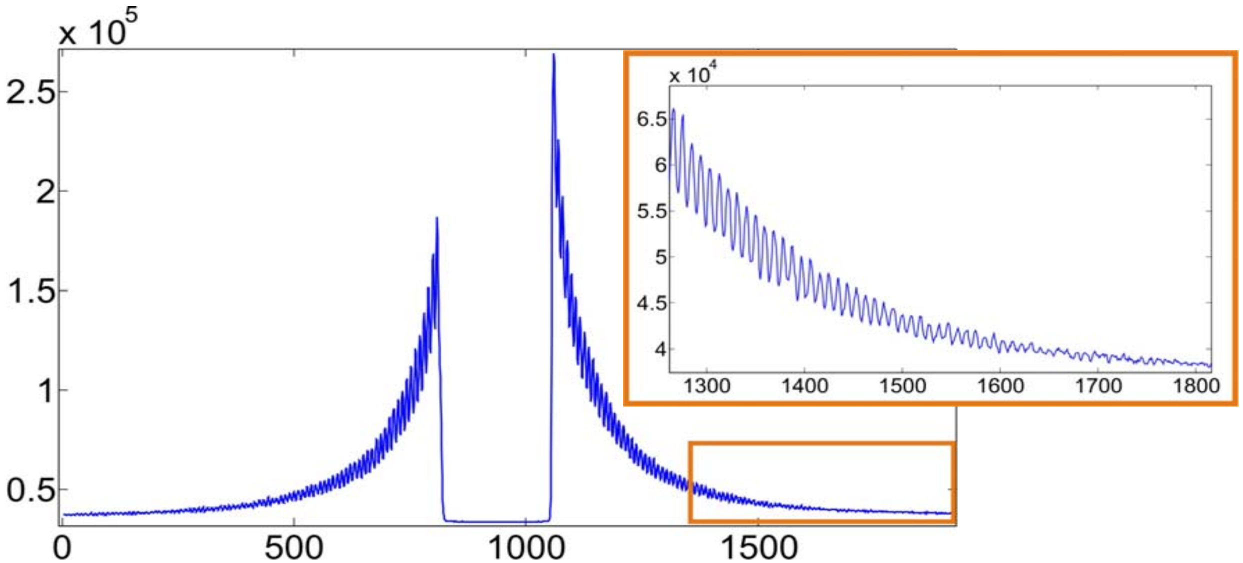

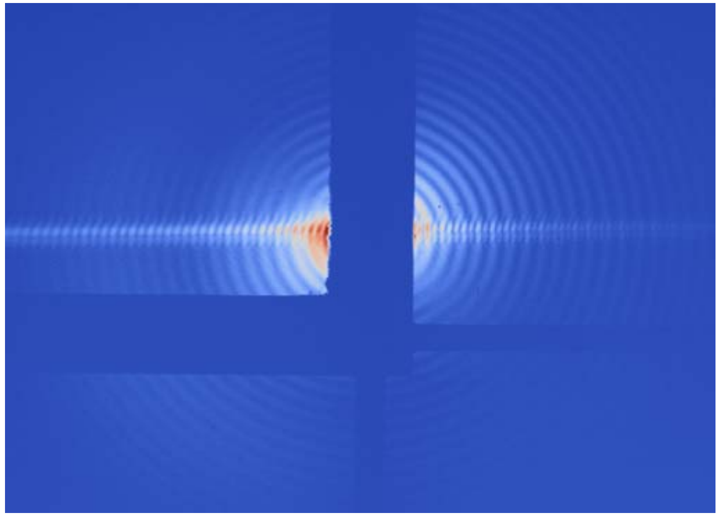

FLASH F-20090335

FLASH experiments : D.D. Mai, T. Reusch, J. Hallmann, TS Vartaniants, A. Mancuso, A. Rosenhahn, A. Singer, J. Gulden, O. Yefanov T. Senkbeil, T. Gorniak, M. Beckers, Rolf Treusch, Stefan Düsterer

the team / collaborations: acknowledgements

Matthias Bartels *waveguide holography, tomography, neural cells and tissues*
Robin Wilke, *phase reconstruction algorithms, ptychography*
Klaus Giewekemeier *phase reconstruction algorithms, ptychography, cellular imaging*
Marius Priebe *cellular imaging and diffraction*
Christian Oldendrowitz *multicellular organisms*
Sebastian Kalbfleisch *waveguide microscope*
Henrike Neubauer, Sven Krüger *waveguide optics and fabrication*
Markus Osterhoff *numerical optics, focusing, mirror design*
Don-Du Mai, Jörg Hallmann, Tobias Reusch *FLASH experiments*

S. Köster, B. Weinhausen Institut für Röntgenphysik
T. Hohage, R. Luke Angew. Mathematik

A. Rosenhahn, U. Heidelberg
M. Sprung, I. Vartanyants, S. Düsterer. R. Treusch DESY
H. Metzger, R. Tucoulou, P. Cloetens ESRF
F. Pfeiffer, A. Diaz, C. Kewish, P. Thibault SLS/ TU München

SFB 755